Unsteady 3D CFD analysis of a 1½-stage turbine with focus on heat transfer validation

Alexander Axelsson

Preface

The work described in this thesis was performed at the Department of Aerothermodynamics at GKN Aerospace Sweden AB in conjunction with the Department of Mechanics at The Royal Institute of Technology. This thesis is the final degree project for the Master's Program in Engineering Mechanics.

I would like to thank my supervisors Jonathan Mårtensson from GKN Aerospace Sweden AB and Lisa Prahl Wittberg from KTH Mechanics for their help and support during the progress of this thesis. I would also like to thank the rest of the people I met at GKN Aerospace Sweden AB for their support and for inviting me to participate in all the social activities.

Abstract

The turbine mid-structure is a component located downstream of the high-pressure turbine in modern turbo-fan engines. It is exposed to high gas temperatures. It is therefore of interest to predict heat transfer in this component. In this thesis unsteady and steady computational fluid dynamics (CFD) simulations carried out with ANSYS CFX are used to predict heat transfer in the turbine mid-structure. Experimental data is used for validation of the results. In one of the unsteady simulations a 90 degree sector of the turbine is used. The other unsteady simulation uses a Transient Blade Row model and a smaller sector of the turbine. At 50% span the simulations underpredict the heat transfer on the pressure side and on the leading edge of the turbine mid-structure vane compared to measurements. On the suction side the agreement with measurements is better. The 90 degree sector simulation does not match the measurements much better than the results of the Time Transformation method and the steady simulation. Further unsteady simulations may advantageously be of the Time Transformation type due to its smaller computational cost.

Nomenclature

Symbol	Unit	Description
a_{ij}	$[m^2/s^2]$	Reynolds-stress anisotropy
h_c	$[W/m^2K]$	Convection heat transfer coefficient
h	$[m^2/s^2]$	Specific enthalpy
h_t	$[m^2/s^2]$	Total specific enthalpy
k	$[m^2/s^2]$	Turbulent kinetic energy
k_{th}	$[W/mK]$	Thermal conductivity
L	$[m]$	Characteristic length
M	$[-]$	Mach number
Nu	$[-]$	Nusselt number
P	$[W]$	Power
p	$[Pa]$	Pressure
$\dot{q}$	$[W/m^2]$	Convective heat flux
$\overline{S}_{ij}$	$[s^{-1}]$	Mean rate-of-strain tensor
s	$[J/K \cdot kg]$	Specific entropy
T	$[K]$	Temperature
T_t	$[K]$	Total temperature
u^+	$[-]$	Dimensionless velocity
u_τ	$[m/s]$	Friction velocity
w_s	$[m^2/s^2]$	Specific shaft work
y^+	$[-]$	Wall coordinate
δ_{ij}	$[-]$	Kronecker delta
δ_ν	$[m]$	Viscous lengthscale
ϵ	$[m^2/s^3]$	Turbulence dissipation rate
γ	$[-]$	Ratio of specific heats
μ	$[Pa \cdot s]$	Dynamic viscosity
ν	$[m^2/s]$	Kinematic viscosity
ν_T	$[m^2/s]$	Turbulent viscosity
ρ	$[kg/m^3]$	Density
τ	$[Nm]$	Torque
τ_w	$[Pa]$	Wall shear stress
ω	$[s^{-1}]$	Turbulence eddy frequency

Contents

1 Introduction

The Department of Aerothermodynamics at GKN Aerospace Engine Systems is currently involved in a number of European projects in which heat transfer in turbine mid-structures is studied. The turbine mid-structure is a component located downstream of the high-pressure turbine in modern turbo-fan engines. It often has both an aerodynamic and a load-carrying function and is exposed to high inlet temperatures. In this thesis work the flow through a turbine has been analyzed using ANSYS CFD tools. Experimental data from a $1^1/_2$-stage turbine at Oxford University was used for validation purposes during the post-processing of the numerical results. Unsteady and steady simulations have been conducted and their results compared. The focus has been on heat transfer validation in the turbine mid-structure.

2 Background

2.1 Gas turbine engines

The layout of a gas turbine jet engine is presented in figure 1. Gas turbines have many applications but they are mainly associated with jet propulsion in aircraft. A jet engine is designed to accelerate large masses of air in one direction and thereby be subject to a net force in the opposite direction. A typical gas turbine engine consists of a compressor, a number of combustion chambers and a turbine. Air from the atmosphere is drawn into the engine and is compressed by the compressor, heated, expanded and accelerated in the combustion chambers and then guided to transfer some of its energy to the turbine blades before entering the exhaust system. The turbine drives the compressor and accessories. The flow through the turbine yields a large negative contribution to the thrust of the engine but the contributions from the compressor and the combustion chamber more than compensate for this. All contributions sum up to a considerable positive net thrust.

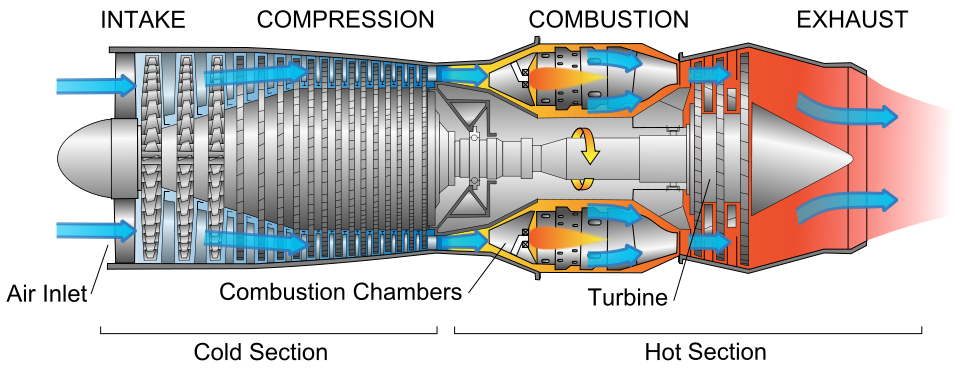

Figure 1: The layout of a turbojet engine [11].

An axial turbine may have several *stages*. Each stage consists of stationary guide vanes

followed by the turbine blades which are free to rotate around the axis of the turbine. As can be seen from figure 1 there are more compressor stages than turbine stages. The reason for this is that the compressor stages are exposed to unfavorable pressure gradients, i.e. the pressure increases in the direction of the flow. By using many compressor stages each compressor stage is exposed to a small increase in pressure and this helps prevent an aggravation of the boundary layer buildup on the blades and endwall surfaces [10, ch. 2].

The components of the turbine are to a various extent exposed to high temperatures which has a degrading effect on them. A turbine may be cooled by air from the compressor but such an arrangement is not considered here [1]. Predicting heat transfer is important when designing the components and Computational Fluid Dynamics is a valuable prediction tool.

2.2 Some facts about turbomachinery

Assuming an isentropic flow through a varying-area passage that either accelerates or decelerates the flow, equations relating the Mach number and the differentials of the pressure, area and fluid velocity can be derived:

$$\frac{dA}{A} = \frac{dp}{p}\left(\frac{1-M^2}{\gamma M^2}\right), \tag{1}$$

$$\frac{dV}{V} = \left(\frac{-1}{\gamma M^2}\right)\frac{dp}{p}. \tag{2}$$

Equations (1) and (2) show that in a subsonic flow ($M < 1$) an increasing area is associated with an increasing static pressure and a decreasing velocity. A decreasing area is associated with a decreasing static pressure and an increasing velocity. In a supersonic flow ($M > 1$) the opposite statements are true.

Applying the principle of conservation of energy across any of the components in a turbomachine, the following equation can be derived:

$$q + w_s = h_{t2} - h_{t1}. \tag{3}$$

In equation (3) q is the heat energy gained by the gas per unit mass, w_s is the exerted shaft work per unit mass and h_t is the *total enthalpy per unit mass*,

$$h_t = h + \frac{V^2}{2}. \tag{4}$$

In (4) h is the static enthalpy per unit mass and V is the local velocity. The subscripts 1 and 2 in (3) refer to inlet and exit stations between which the conservation law is applied, see figure 2. Equation (3) relies on the assumption that the average flow properties prevail along the *pitch line* at some radius between the hub and the shroud. If only the average properties are considered, the flow can be regarded as one dimensional and this is the reason for the simple appearance of equation (3). The simplified analysis that leads to (3) include

the assumption of a steady inviscid flow and the neglect of the effect of a change in potential energy. As opposed to the blade-to-blade passages of a compressor rotor the blade-to-blade passages of a turbine rotor are converging and accelerate the flow. If the flow is approximated as adiabatic, i.e. $q = 0$, equation (3) and (4) show that across a turbine stator ($w_s = 0$) there is a conversion of enthalpy to kinetic energy.

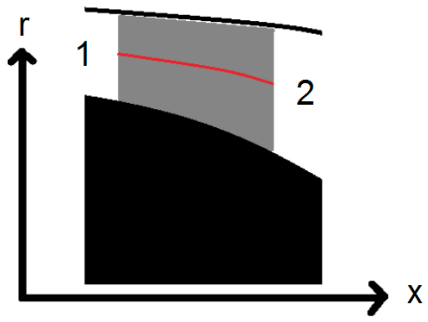

Figure 2: A meridional view of a rotor. The red line is the pitch line.

If the mass-flow rate and the *velocity triangles* (figure 3) are known the torque, power and shaft work produced by the flow can be calculated.

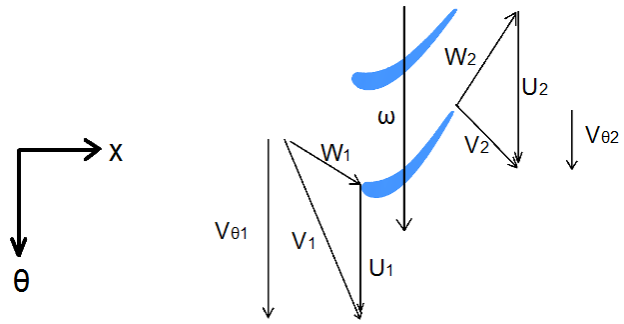

Figure 3

At radius r in a rotor rotating with angular velocity ω the absolute velocity vector, $\mathbf{V}$, of a fluid particle is the sum of the velocity vector relative to a rotor blade, $\mathbf{W}$, and the velocity of the blade, $\mathbf{U} = \omega r\hat{\theta}$:

$$\mathbf{V} = \mathbf{W} + \mathbf{U}. \tag{5}$$

Here $\hat{\theta}$ is the unit vector in the θ-direction. The flow through the rotor produces a net torque, τ, on the shaft resulting from the change in the tangential-velocity component from $V_{\theta 1}$ to $V_{\theta 2}$. This torque is given by

$$\tau = \dot{m}\left(r_1 V_{\theta 1} - r_2 V_{\theta 2}\right) \tag{6}$$

where $\dot{m}$ is the mass-flow rate. It follows that the power absorbed by the rotor is given by

$$P = \omega\dot{m}\left(r_1 V_{\theta 1} - r_2 V_{\theta 2}\right). \tag{7}$$

Dividing the power by the mass-flow rate yields the specific shaft work:

$$w_s = U_1 V_{\theta 1} - U_2 V_{\theta 2}. \tag{8}$$

Equations (6), (7) and (8) are different versions of what is historically known as Euler's 'turbine' equation.

The effect of the fluid viscosity is significant in the vicinity of the solid surfaces and in the wakes downstream of the trailing edges of vanes and blades. In these regions the shear stresses caused by viscosity are predominant. The irreversible viscous dissipation leads to entropy production. Via the principle of conservation of energy and the assumtion of a perfect gas an expression for the entropy production can be derived:

$$\Delta s = c_p \ln\left(\frac{T_{t2}}{T_{t1}}\right) - R \ln\left(\frac{p_{t2}}{p_{t1}}\right) > 0, \tag{9}$$

where 1 refers to the initial state and 2 to the second state and R is the ideal gas constant. The *total temperature*, T_t, is related to the fluid velocity, V, and the specific heat under constant pressure, c_p, via

$$T_t = T + \frac{V^2}{2c_p}. \tag{10}$$

The *total enthalpy* is related to the total temperature via

$$h_t = c_p T_t. \tag{11}$$

In an ideal gas c_p is temperature dependent. However, across a separate turbomachinery stage it is customary to work with an averaged value of c_p. It is thus possible to express equation (3) in the following way:

$$q + w_s = c_p(T_{t2} - T_{t1}). \tag{12}$$

From (12) it is clear that across an adiabatic stator ($q = 0$, $w_s = 0$) the total temperature is constant and the first term in equation (9) therefore vanishes. Thus for the flow across an adiabatic stator the loss in total pressure can be related to an increase in entropy due to e.g. frictional effects [10, ch. 3,4].

2.3 Heat transfer

Heat transfer is induced by a spatial temperature difference. One distinguishes between three types of processes through which heat is transferred: *conduction*, *radiation* and *convection*. Conduction is the transfer of energy from particles with higher internal energy to particles with lower internal energy due to interactions between the particles. Radiation is caused by changes in the electron configurations of the atoms of the emitting matter. Electromagnetic waves transport the energy of the radiation field. Unlike conduction and convective heat

transfer, radiation transfer can occur in vacuum. Convection is the most important process in this thesis. It is the superposition of the heat transfer by diffusion of energy at a molecular level and by the bulk motion of the fluid, i.e. the superposition of conduction and advection. A relation called *Newtons law of cooling* is employed when quantifying the convective heat flux across a solid surface:

$$\dot{q} = h_c \cdot (T_s - T_{ref}), \tag{13}$$

where $\dot{q}$ is the convective heat flux (W/m^2), h_c is the convective heat transfer coefficient (W/m^2K) and T_s and T_{ref} are the surface temperature and fluid reference temperature respectively. The convective heat transfer coefficient depends on several flow properties. Important fluid properties include thermal conductivity, specific heat, density and viscosity. The profiles of the thermal and velocity *boundary layers* greatly influence the wall heat flux and shear stress. A laminar velocity boundary layer profile on a flat plate is presented in figure 4.

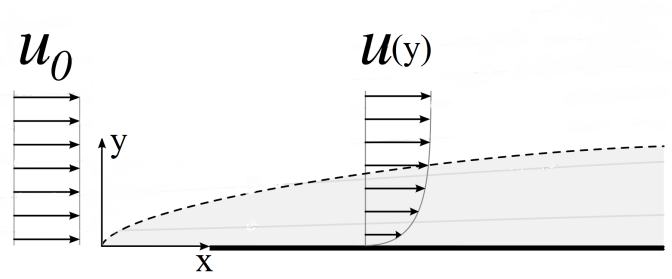

Figure 4: The development of a boundary layer on a flat plate [12].

Fluid particles in contact with the plate surface have zero velocity. These fluid particles impede the motion of passing fluid particles through shear forces. The passing fluid particles in turn impede the motion of the fluid particles at greater distance y from the plate surface and so on. This causes a boundary layer to form where the velocity in the x-direction, $u(y)$, increases with y until reaching the freestream velocity u_0 outside the boundary layer. Similarly a thermal boundary layer will form if the plate surface is at a different temperature than the freestream flow. Fluid particles in contact with the plate surface will achieve thermal equilibrium at the plate temperature. Temperature gradients will develop in the fluid and heat is exchanged between fluid particles throughout the thermal boundary layer.

The heat flux at a solid boundary is proportional to the temperature gradient at that boundary. Whether the boundary layer is turbulent or laminar will affect the magnitude of the heat flux [4, ch. 1].The majority of flows in nature and in engineering applications are turbulent. Opposed to laminar flows turbulent flows are characterized by chaos and unpredictability. Other features of turbulence are a wide spectrum of scales of eddies, a large Reynolds number and diffusivity. Kinetic energy is transferred in a cascade process from big scales to increasingly smaller scales and finally dissipated into heat [3]. Three main regions in a turbulent boundary layer may be defined. In the outer region transport is dominated by turbulent mixing. In the next region, the *buffer layer*, turbulent mixing and diffusion are of the same order. The innermost region is called the *viscous sublayer*, where diffusion is the dominating

mode of transport. For a given free stream velocity both the velocity gradient and temperature gradient are larger close to the wall in a turbulent boundary layer compared a laminar boundary layer. This implies that the wall shear stress and heat transfer coefficients are larger in a turbulent boundary layer. Figure 5 shows sketches of one mean turbulent velocity boundary layer and one laminar velocity boundary layer profile on a flat plate with the same free stream velocity at the same distance from the leading edge of the plate. It illustrates that at the wall the velocity gradient of the mean turbulent boundary layer profile is larger than the gradient of the laminar profile.

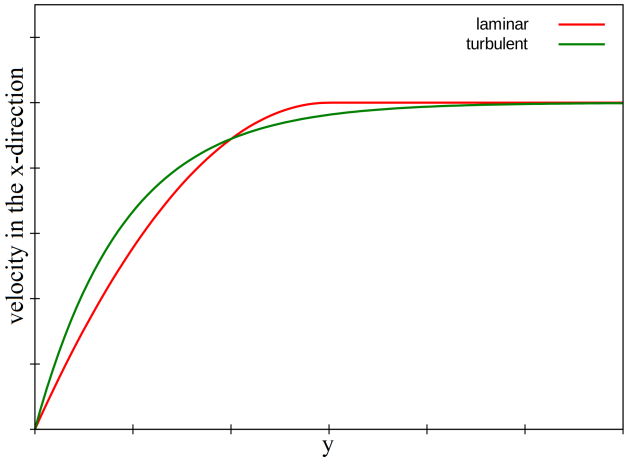

Figure 5: Comparison between a turbulent and a laminar boundary layer profile [13].

An important dimensionless parameter in the context of heat transfer is the *Nusselt number* defined by

$$Nu = \frac{hL}{k}, \tag{14}$$

where h is the convective heat transfer coefficient, L a characteristic length and k the thermal conductivity. The Nusselt number is equal to the dimensionless temperature gradient evaluated at the wall and can be interpreted as the ratio of convective to conductive heat transfer [4, pp. 360-376].

The regions of the flow near walls can be more precisely defined on the basis of the non-dimensional wall distance, y^+, defined by

$$y^+ \equiv \frac{y}{\delta_\nu}, \tag{15}$$

where the *viscous lengthscale*, δ_ν, is defined by

$$\delta_\nu \equiv \nu \sqrt{\frac{\rho}{\tau_w}}. \tag{16}$$

The above expression contains the *wall shear stress*, τ_w, given by

$$\tau_w \equiv \mu \left. \frac{d \langle U \rangle}{dy} \right|_{y=0}, \tag{17}$$

where y is the distance from the wall. In particular for channel flow, a flow confined in a rectangular channel, the viscous sublayer extends to around $y^+ = 5$ and the next region, the buffer layer, extends to around $y^+ = 30$. Beyond the buffer layer, extending from $y^+ = 30$ up to $y/\delta = 0.3$ where δ is the channel half height, there is a region called the *log-law region* where the following expression for the non-dimensional velocity, u^+, holds

$$u^+ = \frac{1}{\kappa} \ln y^+ + B. \tag{18}$$

The reported values of the von Kármán constant κ and B vary in the literature but are typically within 5% of 0.41 and 5.2 respectively [5, pp. 268-276]. The non-dimensional velocity u^+ above is defined by

$$u^+ \equiv \frac{\langle U \rangle}{u_\tau}, \tag{19}$$

where u_τ, the *friction velocity*, is given by

$$u_\tau \equiv \sqrt{\frac{\tau_w}{\rho}}. \tag{20}$$

2.4 Computational fluid dynamics

Computational fluid dynamics is the science concerned with solving the equations governing fluid motion numerically [2, p. 411]. The equations are discretized through some technique and thereby converted to a system of algebraic equations which is solved with the help of computers. The values of the solution variables are computed using discrete spatial points and control volumes in the domain where the equations are solved. All those discrete points and their connections constitute the *mesh*, also called the grid. Several sources of error affect CFD predictions. Discretizing the equations introduces discretization errors. These errors grow with the time step and the spacing between grid points. The effect of discretization errors on the solution can be assessed by performing a grid convergence study. This amounts to comparing results obtained from successively refined grids. If the value of a parameter of interest, e.g. drag coefficient, changes negligibly as the number of grid points is increased the parameter is becoming independent of the number of grid points [9, p. 207]. The time step may need to be studied in a similar fashion. In practice grids cannot be arbitrarily fine since the computational effort will increase with the number of grid points. Besides the number of gridpoints and their distribution in a grid, the geometrical properties of the grid cells also affect accuracy and convergence. The degree to which the solution is converged is an additional source of error. Residuals and flow variables should be monitored during a simulation to avoid halting it before it has converged. There are other sources of errors besides discretization errors. The geometry of the domain is an approximation of the real geometry. Finer details e.g. cavities in the hub between rotating and stationary components

might be neglected and surfaces represented as perfectly smooth. Inlet and outlet boundary conditions may also be approximations of the real ones. Furthermore the physical models used for describing the flow may not be absolutely accurate. One important example of modeling in CFD is turbulence modeling which is discussed in section 2.4.2 [9, pp. 205, 235-238].

The Finite Volume Method is a widely used method by which the governing flow equations are discretized. A small control volume is associated to each grid point in the domain. The integral forms of the governing equations are discretized and applied to each of these control volumes. An advantage with the Finite Volume Method is that global conservation of flow variables is satisfied automatically [14, ch. 5].

2.4.1 The governing equations

The governing equations in fluid dynamics enforce conservation of mass, momentum and energy. For an arbitrary fixed control volume Ω bounded by a closed surface S the mass conservation equation reads

$$\frac{\partial}{\partial t}\int_{\Omega}\rho d\Omega + \oint_{S}\rho\vec{v}\cdot d\vec{S} = 0, \tag{21}$$

where ρ is the fluid density and $\vec{v}$ is the fluid velocity. The first term represents the change of mass in the control volume per time. The second term represents the mass flow rate out of from the surface S. A general form of the momentum equation reads

$$\frac{\partial}{\partial t}\int_{\Omega}\rho\vec{v}d\Omega + \oint_{S}\rho\vec{v}\left(\vec{v}\cdot d\vec{S}\right) = \int_{\Omega}\rho\vec{f_e}d\Omega + \oint_{S}\overline{\overline{\sigma}}\cdot d\vec{S}. \tag{22}$$

Here $\vec{f_e}$ is the sum of external forces per unit volume and mass and $\overline{\overline{\sigma}}$ is the internal stress tensor. The first term in (22) represents the time rate of change in momentum of the fluid inside the control volume. The second term represents the momentum flow rate out from the bounding surface of the control volume. The terms on the right-hand side represent contributions from volume and surface forces to the total force acting on the control volume. Finally the energy equation reads

$$\frac{\partial}{\partial t}\int_{\Omega}\rho E d\Omega + \oint_{S}\rho E\vec{v}\cdot d\vec{S} - \oint_{S}k\nabla T\cdot d\vec{S} = \int_{\Omega}\left(\rho\vec{f_e}\cdot\vec{v} + q_H\right)d\Omega + \oint_{S}\left(\overline{\overline{\sigma}}\cdot\vec{v}\right)\cdot d\vec{S} \tag{23}$$

$E = e + \vec{v}\cdot\vec{v}/2$ is the total energy per unit volume and unit mass. The vector quantities $\rho E\vec{v}$ and $-k\nabla T$ are the convective and diffusive fluxes of energy respectively. Heat sources such as radiation and heat released by chemical reactions per unit time and volume are designated by q_H. The expression $\rho\vec{f_e}\cdot\vec{v}$ represents the work of the volume forces per unit time and unit volume. The expression $\overline{\overline{\sigma}}\cdot\vec{v}$ represents the work done per unit time and unit area on the fluid by the internal shear stresses acting on the surface of the control volume. Thus the terms on the left-hand side in equation (23) represent the time rate of change in total energy and the flow of energy out from the surface of the control volume. The terms on

the right-hand side represent contributions to the time rate of change in total energy from volume forces, surface forces and other heat sources.

To close the system of equations it must be supplemented with constitutive relations. The pressure and/or temperature dependence of the internal energy and viscosity must also be specified [14, ch. 1].

2.4.2 Turbulence modeling

In a *direct numerical simulation* (DNS) the discretized governing equations are solved without any modelling of turbulence. It requires all the length and time scales to be resolved. It is the most accurate type of simulation but also the most computationally expensive. The computational effort increases approximately as the cube of the Reynolds number and most of it is spent on the smallest, dissipative motions. There are examples where a DNS can provide accurate information more successfully than an experiment [5, p. 357]. Because of its computational cost the DNS is not used for industrial applications.

Large-eddy simulation (LES) is more suitable for some industrial applications as it is less expensive. In contrast to DNS the smaller scales of motion are modeled in LES and this saves computational cost. In LES the velocity field $\boldsymbol{U}(\boldsymbol{x},t)$ is decomposed into a filtered (or resolved) component $\overline{\boldsymbol{U}}(\boldsymbol{x},t)$ and a residual (or subgrid-scale) component $\boldsymbol{u'}(\boldsymbol{x},t)$: $\boldsymbol{U}(\boldsymbol{x},t) = \overline{\boldsymbol{U}}(\boldsymbol{x},t) + \boldsymbol{u'}(\boldsymbol{x},t)$. The filtered component is an approximation to the large-scale motions of the flow. With this decomposition equations for the filtered velocity can be derived from the Navier-Stokes equations. The equations for the filtered velocity contain the residual stress tensor that needs to be modeled for example by a turbulent-viscosity model. Opposed to the RANS models described next LES captures the unsteady large-scale turbulent structures and can be used to study aeroacoustics [5, pp. 559-559, 635-638].

In industrial applications it is common to solve the equations describing average quantitites and thereby obtain less detailed but adequate information about the flow field variables. This approach is much cheaper than DNS and LES but is also less accurate and it involves more modelling.
For compressible flows the averaging is weighted by density and results in the so called Favre-averaged Navier-Stokes equations. Compressibility effects are certainly not negligible in the turbine studied in this thesis but for purpose of illustration the *Reynolds-averaged Navier-Stokes equations* that describe an incompressible flow are presented:

$$\frac{\bar{D}\left\langle U_j\right\rangle}{\bar{D}t} = \nu\nabla^2\left\langle U_j\right\rangle - \frac{\partial\left\langle u_i u_j\right\rangle}{\partial x_i} - \frac{1}{\rho}\frac{\partial\left\langle p\right\rangle}{\partial x_j}, \text{where } \frac{\bar{D}}{\bar{D}t} \equiv \frac{\partial}{\partial t} + \langle\boldsymbol{U}\rangle \bullet \nabla \tag{24}$$

Quantities within brackets denote mean (averaged) values. The Reynolds equations are derived by decomposing the velocity field into its mean and the fluctuation from the mean, $\boldsymbol{U}(\boldsymbol{x},t) = \langle\boldsymbol{U}(\boldsymbol{x},t)\rangle + \boldsymbol{u}(\boldsymbol{x},t)$, and then taking the average of the incompressible Navier-Stokes equations:

$$\frac{D\boldsymbol{U}}{Dt} = -\frac{1}{\rho}\nabla p + \nu\nabla^2\boldsymbol{U}. \tag{25}$$

A modified pressure, p, is used in these equations, equal to the sum of the pressure and the gravitational potential multiplied by the density. Clearly the only difference between the Reynolds equations and the Navier-Stokes equations is the term $-\frac{\partial \langle u_i u_j \rangle}{\partial x_i}$. The expression $\langle u_i u_j \rangle$ is called *Reynolds stresses*. The Reynolds equations along with the mean continuity equation,

$$\nabla \bullet \langle \boldsymbol{U} \rangle = 0, \tag{26}$$

are the governing equations for the mean velocity field. Thus there are four equations but due to the Reynolds stresses more than four unknowns. To close the equation system the Reynolds stresses need to be determined.

On way of dealing with this problem is to resort to the *turbulent-viscosity hypothesis* described below. Another approach is to solve transport equations for the Reynolds stresses and for a time or length scale determining quantity like ω or ϵ. These *Reynolds-stress models* do not rely on the turbulent-viscosity hypothesis but the transport equation for the Reynolds stresses contains terms that must be modeled [5, pp. 387-462].

According to the turbulent-viscosity hypothesis the *Reynolds-stress anisotropy* defined by $a_{ij} \equiv \langle u_i u_j \rangle - \frac{2}{3} k \delta_{ij}$ is aligned with the *mean rate-of-strain* tensor, $\overline{S}_{ij} \equiv \frac{1}{2}\left(\frac{\partial \langle U_i \rangle}{\partial x_j} + \frac{\partial \langle U_j \rangle}{\partial x_i}\right)$. This can be expressed as

$$-\rho \langle u_i u_j \rangle + \frac{2}{3}\rho k \delta_{ij} = 2\rho \nu_T \overline{S}_{ij}, \tag{27}$$

where the turbulent kinetic energy is defined by

$$k \equiv \frac{1}{2} \langle u_l u_l \rangle \tag{28}$$

and δ_{ij} is the Kronecker delta. ν_T is the *turbulent viscosity*. Relation (27) is analogous to the relation for the viscous stress in a Newtonian fluid (see e.g. [2] pp. 100-103):

$$\frac{-(\tau_{ij} + p\delta_{ij})}{\rho} = -2\nu S_{ij} \tag{29}$$

where τ_{ij} is the stress tensor and $S_{ij} = \frac{1}{2}\left(\frac{\partial u_i}{\partial x_j} + \frac{\partial u_j}{\partial x_i}\right)$ is the strain rate tensor. Substituting the turbulent-viscosity relation into the mean-momentum equation (24) yields

$$\frac{\bar{D}}{\bar{D}t} \langle U_j \rangle = \frac{\partial}{\partial x_i}\left[\nu_{\text{eff}}\left(\frac{\partial \langle U_i \rangle}{\partial x_j} + \frac{\partial \langle U_j \rangle}{\partial x_i}\right)\right] - \frac{1}{\rho}\frac{\partial}{\partial x_j}\left(\langle p \rangle + \frac{2}{3}\rho k\right). \tag{30}$$

where the *effective viscosity* is given by

$$\nu_{\text{eff}} = \nu + \nu_T(\boldsymbol{x}, t). \tag{31}$$

The above equations have the same form as the Navier-Stokes equations (25). They can be solved if ν_T is specified. The turbulent-viscosity hypothesis and relation (27) solves the

problem of having more unknowns than equations. It is however not generally valid in all types of flow. Nonetheless the popular turbulent-viscosity turbulence models rely on this hypothesis [5, pp. 83-95, 358-365].

The $k-\omega$ SST turbulence model used in the simulations described in this report is an example of a *two-equation model.* In such a model two equations describing the transport of two turbulent quantities are solved. The two turbulent quantities are then used to form an expression for ν_T and hence make it possible to solve (30). The turbulent quantities involved in the $k-\omega$ model is the turbulent kinetic energy, k, the turbulence dissipation rate , ε, and the turbulence frequency defined by $\omega \equiv \varepsilon/k$ [5, pp. 373-385]. These are used to calculate ν_T [6, ch. 2]:

$$\nu_T = \frac{k}{\omega}. \tag{32}$$

2.5 Flow solver

ANSYS CFX was used for solving the discrete set of equations for the flow through the turbine. It is a commercial CFD program developed by ANSYS Inc and is widely used in many different industrial applications. It implements finite volume discretizations of the governing equations (the continuity equation, the momentum equation and the energy equation) which are solved together with the constitutive relations. The discretizations are mostly of second order accuracy. Finite-element shape functions are used to describe how variables vary within a mesh element.

2.5.1 Residuals and Auto timescale

The application of the finite-volyme method to all the mesh elements in the domain gives rise to a linear equation system which can be written in the form

$$Ax = b, \tag{33}$$

where A is the coefficient matrix, x the solution vector and b the right hand side. In general such a system can solved iteratively by starting with an approximate solution, x^n, and letting the improved solution vector at the next iteration step be given by

$$x^{n+1} = x^n + x', \tag{34}$$

where x' is given by

$$Ax' = r^n. \tag{35}$$

The *residual*, r^n, is given by

$$r^n = b - Ax^n. \tag{36}$$

Repeating these steps would produce an increasingly accurate solution vector. The residuals monitored during a CFX simulation are normalized with representative ranges of the flow

variables in the domain [6, ch. 11.2].

During a steady-state simulation the equations are under-relaxed by applying a 'false time step'. This time step can be adjusted too speed up convergence. Several options for controlling the time scale on which the time step is based are available. The *Auto Timescale* option uses an internally calculated physical time scale based on the conditions of the flow. The speed of the convergence can be increased by increasing the *Time Scale Factor*[7, ch. 15.4]. A time scale in the interval $0.1/\omega$ to $1/\omega$ is recommended for gas turbine applications where ω is the angular velocity of the rotor [8, ch. 11].

CFX employs an implicit time discretization scheme and in transient simulations a number of coefficient loops are performed to advance in time. Three to five loops per timestep are recommended for most cases [7, ch. 15.4]. Since CFX is an implicit solver the Courant number does not have to be close to one to ensure stability.

2.5.2 The $k-\omega$ turbulence models and wall functions

In gas turbine applications the $k-\omega$ SST turbulence model is a good choice according to the ANSYS 14.5 Reference Guide [8, ch. 11.1.1]. It captures boundary layers and flow separation comparatively accurately. It includes a blending function that makes it behave like a standard $k-\omega$ model within boundary layers and a $k-\epsilon$ model outside boundary layers [7, ch. 4.1.5]. The standard (Wilcox) $k-\omega$ model is more accurate and robust near walls compared to the $k-\epsilon$ model. A drawback is its 'sensitivity to freestream conditions': the results can vary significantly depending on the value of ω specified at the inlet. This is the motivation for the blending of the $k-\omega$ model with the $k-\epsilon$ model that is implemented in the baseline $k-\omega$ model and the SST model in CFX. The advantage of the SST model over the baseline model is that the SST model predicts the onset of separation better [6, ch. 2.2]. Another advantage with the ω based models in CFX is the *Automatic Wall Treatment* feature available for them. If the near-wall grid resolution gets sufficiently low, the solver will automatically switch to wall functions if Automatic Wall Treatment is enabled.

A major fraction of the total number of grid points will be needed in the near-wall region if the steep gradients there are to be resolved. If wall functions are used the turbulence-model equations are not solved in the immediate vicinity of the wall. Instead boundary conditions based on log-law relations are applied at the wall adjacent nodes which should be placed in the log-law region. The turbulence-model equations are solved with these boundary conditions outside the region between the wall and the wall adjacent nodes [5, p. 442].

2.5.3 The Time Transformation method and the Stage interface

The *Profile Transformation* and *Time Transformation* methods of ANSYS CFX were used in some of the transient simulations conducted in this work. These methods make it possible to simulate the flow between rotating and stationary domains that have an unequal pitch. The Profile Transformation scales the flow profile from one domain into the other over the

interface. This results in flow disturbances entering the other domain with an incorrect frequency since the scaling is only spatial but not temporal. When using the Time Transformation method disturbances have the correct frequency as time is also scaled [6, ch. 4].

In CFX the mixing-plane type of interface is called *Stage* interface. This type of interface was used in the steady simulations. It has an ability to simulate blade movement. The flow between rotating and stationary components is treated by changing the frame of reference and the fluxes from the upstream domain are circumferentially averaged in bands and then transmitted to the downstream domain [8, ch. 11.4].

3 Meshing and Simulation Setup

Figures 6 and 7 and show the 1½-stage turbine studied in this thesis. Focus is put on the second stator, referred to as the turbine mid-structure (TMS).

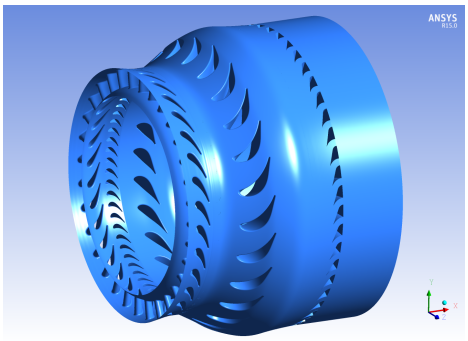

Figure 6: The studied turbine. The outer surface is called *shroud* or *casing* and the inner surface is called *hub*. The flow path is in the space between the hub and the shroud. A component called *deswirler* is located downstream of the turbine in the test rig and in the CFD simulations.

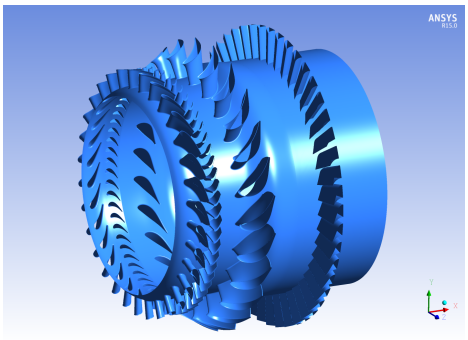

Figure 7: The turbine and deswirler without the shroud. From left to right are the stator vanes, rotor blades, the TMS vanes and finally the deswirler vanes. There are 32 stator vanes, 60 rotor blades, 24 TMS vanes and 48 deswirl vanes.

3.1 Meshing

ANSYS ICEM 15.0 was used for meshing. Structured body-fitted meshes with hexahedra cells were used. Four meshes were available at the start of the work, one for each component. In order to conduct a transient simulation with a one-to-one pitch ratio a minimum of eight stator components, fifteen rotor components and six TMS components are required. These can be arranged in a 90 degree sector of a whole wheel. The computational effort is much greater compared to a steady simulation. To reduce the total number of grid points the mesh density was reduced in the stator and rotor meshes. The near-wall resolution was decreased with the intention to take advantage of the *Automatic Wall Treatment* functionality available for the k-ω SST turbulence model in CFX. The mesh density in the TMS was kept higher since the ambition was to have a y^+ less than one to capture heat transfer more accurately with a resolved boundary layer. The deswirler mesh was kept comparatively coarse since the details of the flow in the deswirler were of small interest in this work.

In the stator mesh the shapes of the blocks around the trailing edge were slightly changed to align the mesh better with the wake, see figure 8 below.

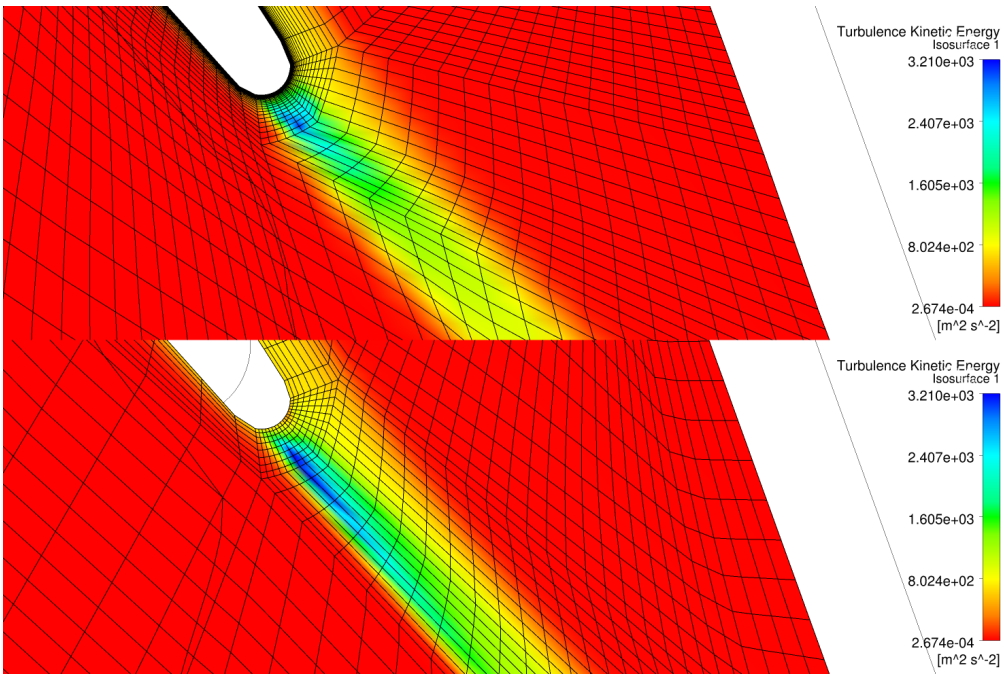

Figure 8: The wake region in the stator before and after changing the blocks.

A concern was whether the wake from the stator could be captured on its way into the TMS domain.

For the generation of rotor meshes with different densities the original block structure of the rotor mesh seemed slightly problematic. Changing parameters of certain edges when attempting to change the mesh density uniformly would result in a region on the suction side with extremely deformed cells. Meshes with a slightly changed block structure were

created to solve this problem, see figure 9. However, time did not permit simulations with these meshes. Therefore only the mesh with the original block structure was used.

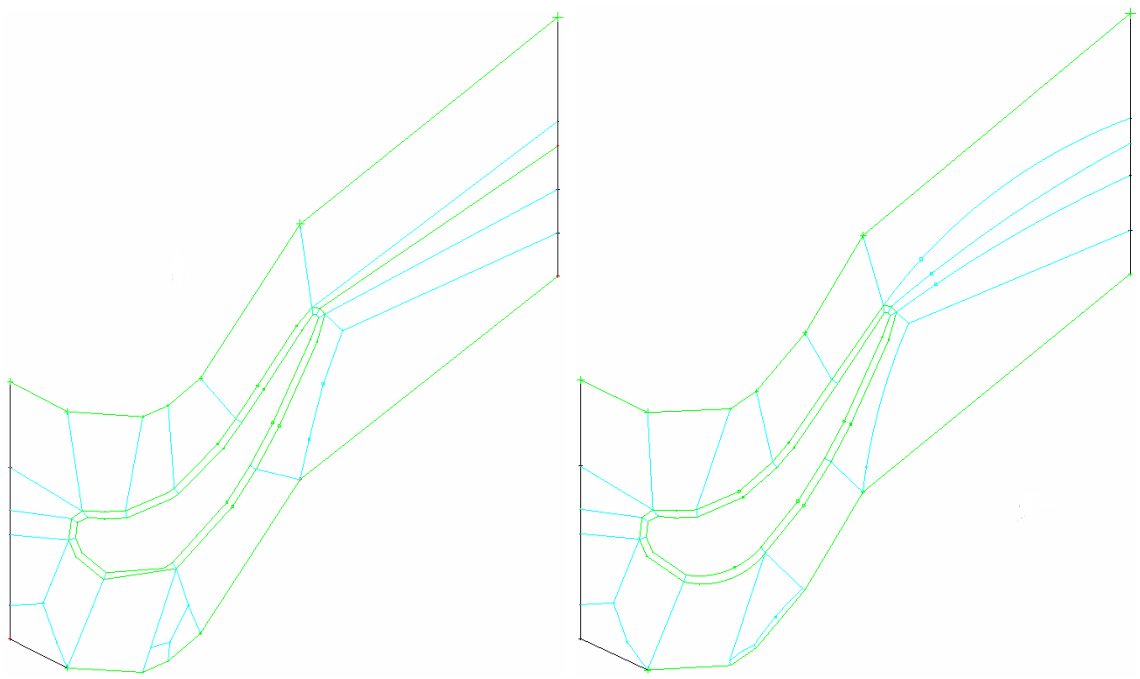

Figure 9: Small changes were made on the blocks in the rotor mesh for future refinement and coarsening. The left picture shows the original blocking and the right picture shows the modified one. The intention was to use the modified blocking to investigate the dependence of the results on the rotor mesh density.

When changing the mesh density the quality of many cells may deteriorate. Improving the quality parameters can be time consuming. Guidelines for minimum values of parameters like angle, determinant, volume change etc. were provided by GKN Aerospace best practice guidelines. Fulfilling the criterion for angle proved difficult in the stator mesh. Figure 10 shows the problematic areas.

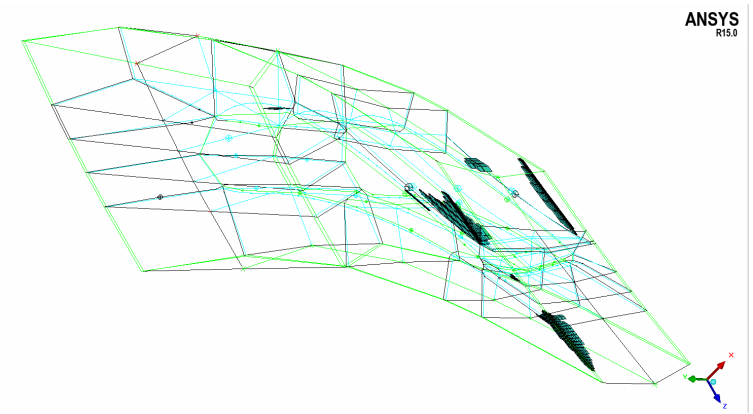

Figure 10: Cells in the stator mesh with angle slightly below the recommended minimum.

The most problematic quality parameter in the TMS is the aspect ratio of the cells. The requirement to have $y^+ < 1$ is difficult to achieve without having high aspect ratio cells close to the walls. During the initial simulations the maximum aspect ratio in the TMS was more than ten times higher than recommended. It was believed this could have a negative influence on the accuracy of the heat transfer predictions in those simulations.

The deswirler mesh has cells with low angle. These cells can be seen in figure 11 below.

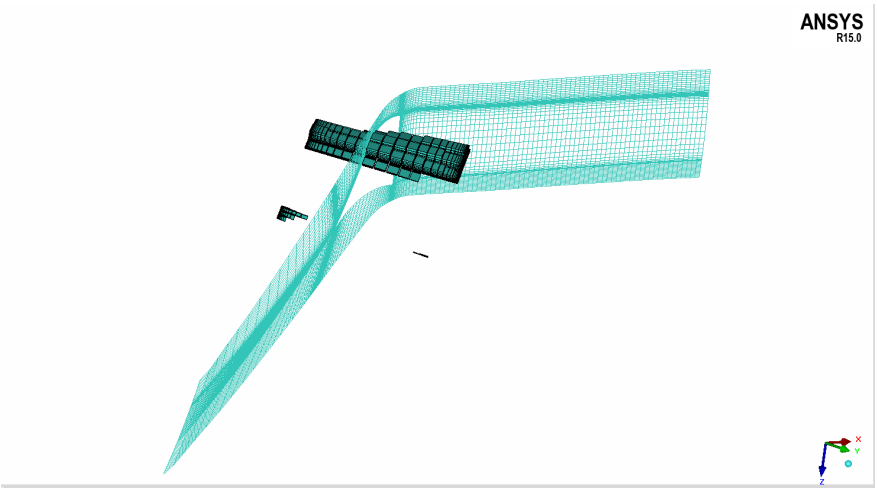

Figure 11: Cells in the deswirler mesh with angle below the recommended minimum.

Side views in the negative radial direction of the meshes for the four components are presented below.

Figure 12: From upper left to lower right: stator, rotor, TMS and deswirler.

Two refined versions of the TMS mesh were created and used in steady simulations. The original TMS mesh has 2.0 million cells and the refined versions have 7.1 million cells and 16.6 million cells respectively. The aspect ratio of near-wall cells in the original mesh is higher than the recommended maximum, especially on the pressure side near the trailing

edge of the vane. In order to improve these aspect ratios in the finer meshes the number of nodes on the edges were not all increased by the same factor. As the y^+ was found to be less than one with the original mesh, the distances between the walls and the first nodes were deemed small enough and therefore not changed.

3.2 Simulation Setup

ANSYS CFX 15.0 and CFX 14.5 were used for the simulations. The angular velocity of the rotor and the total temperature and total pressure at the stator inlet were specified according to the conditions in the test rig. During simulations the static pressure at the deswirler outlet was adjusted to attain the same mass flow rate and same average pressure upstream of the deswirler vane as measured in the test rig. Figure 13 shows where flow variables were monitored in the TMS and deswirler. The monitored variables included pressure, total pressure, temperature, total temperature and the Mach number.

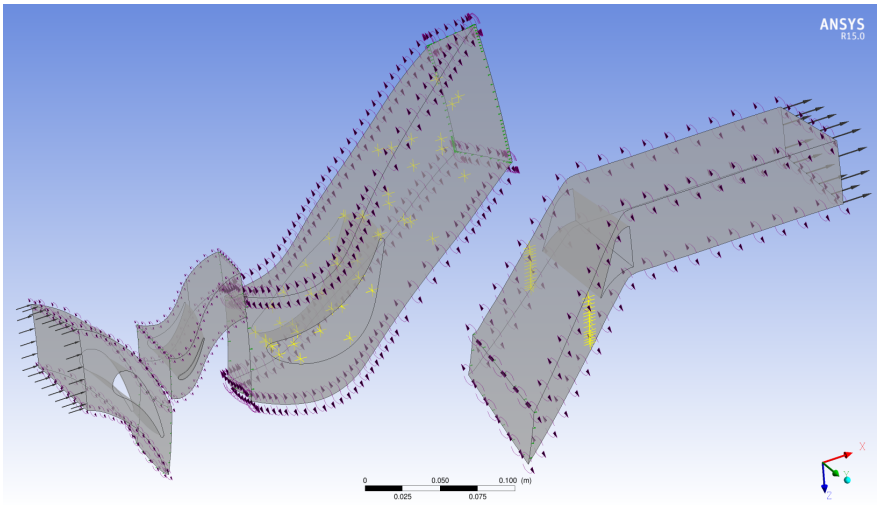

Figure 13: The setup of the steady state simulation. The yellow crosses mark the positions where flow variables were monitored. Total mesh size: 3.2 million cells.

3.3 Monitoring convergence

To help assess convergence in the steady simulations and in the 90 degree unsteady simulations the integral of the *Wall Heat Flux* on the TMS vane was monitored. The steady simulations were not stopped until the monitored values and residuals had become steady. The time scale factor was adjusted to decrease the residuals and the periodic fluctuations in the simulations. Transient simulations were deemed converged when the residuals had become steady and the monitored variables had become periodic with a constant amplitude and a period equal to the time needed for a rotor blade to move one rotor blade pitch. The timestep used in the transient simulations was this time period divided by 30. Five coeffi-

cient loops were performed before updating the position of the rotor.

With the Time Transformation method it is only possible to monitor point values. The integral of the wall heat flux could therefore not be monitored during the Time Transformation simulations. Convergence of the Nusselt number distribution was ensured by confirming that the result from one simulation was close to the result of a simulation that had been running for a longer simulation time.

The steady simulations were carried out with only one of each component as shown in figure 13. Source terms for the turbulence frequency, ω, were specified at the downstream side of the stage interfaces to correct an unphysical jump in ω that may occur across Stage interfaces in CFX. No transition model was used, a fully turbulent flow was assumed.

Figure 14 shows the setup of the 90 degree unsteady simulation.

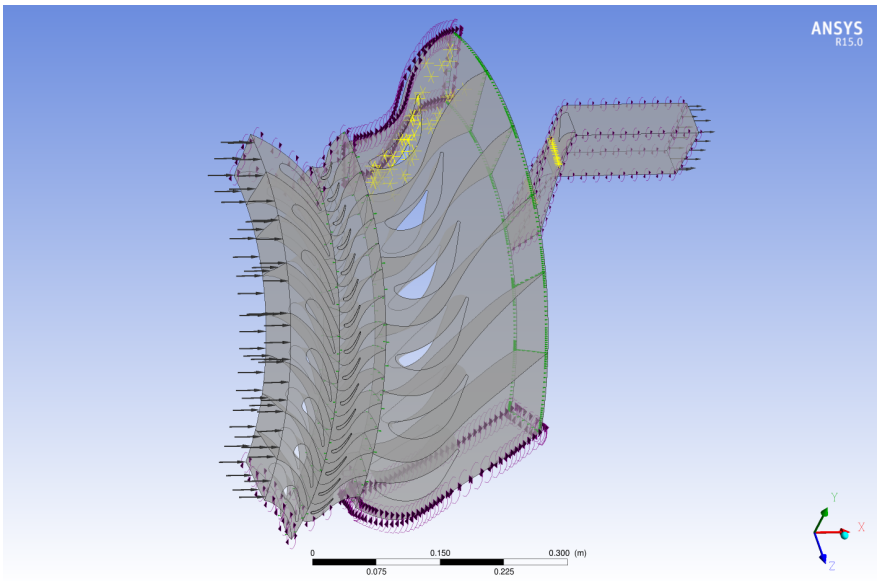

Figure 14: The setup of the 90 degree transient simulation. Total mesh size: 24.8 million cells.

In the transient simulations of the 90 degree sector of the turbine a Stage interface was used between the TMS domain and the deswirler domain. This simulation is expected to give more accurate results but it is much more computationally expensive compared to the Time Transformation method.

Figure 15 shows the Time Transformation setup. The number of components and the total mesh size is drastically reduced compared to the 90 degree simulation.

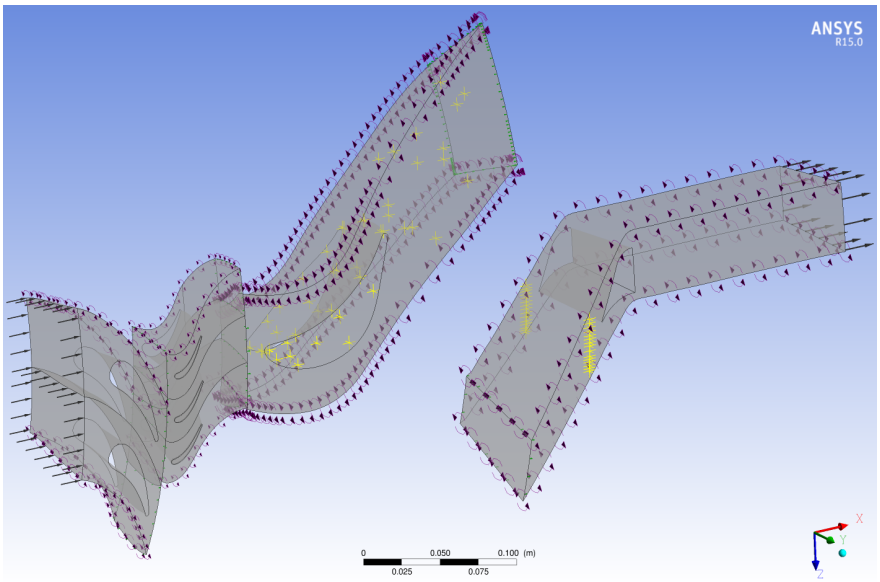

Figure 15: The setup of the Time Transformation simulation. Total mesh size: 4.9 million cells. Two stator vanes, three rotor blades, one TMS vane and one deswirler vane was included.

The reference temperatures needed for calculating the heat transfer coefficent and the Nusselt number on the the TMS vane were obtained from simulations with adiabatic walls in the TMS domain. The heat transfer coefficient was computed by dividing the obtained wall heat flux by the difference between the obtained adiabatic wall temperature and the specified wall temperature. The Nusselt number was calculated from (14), where the chord length of a TMS vane was chosen as the characteristic length. The value of the thermal conductivity in (14) was the same as the one used for the experimentally obtained Nu.

4 Results

All of the Nusselt number distributions presented below are from the curve at 50% span, shown in green in figure 16. The subject of heat transfer measurements in turbines is treated by e.g. Doorly & Oldfield, Oldfield and Piccini [15][16][17].

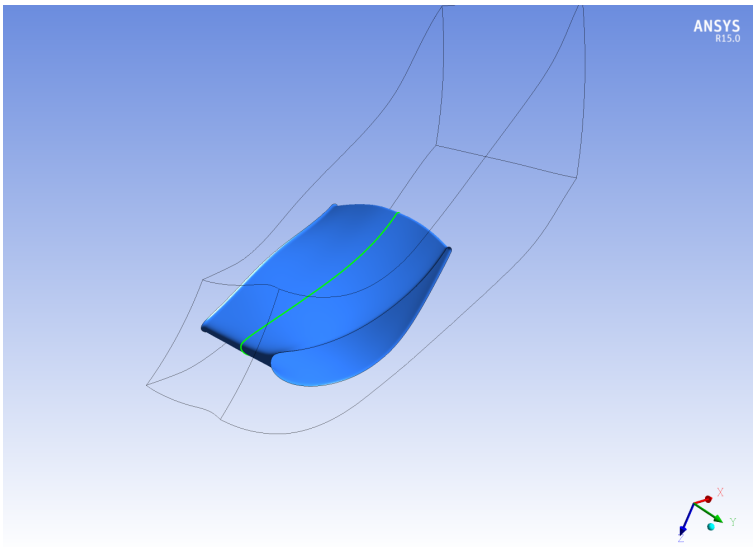

Figure 16: The line from which the Nusselt number distributions shown in this report are extracted.

4.1 Convergence

The RMS residuals typically reached steady values between $3 \cdot 10^{-4}$ and $8 \cdot 10^{-6}$. By adjusting the time scale factor the fluctuating behaviour of the residuals could be reduced as is shown in figure 17.

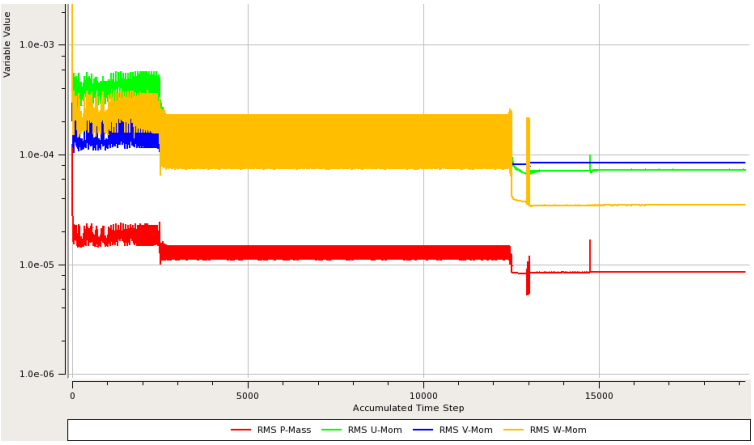

Figure 17: The time scale factor was increased around iteration 13000. The residuals decreased and their fluctuating behaviour attenuated.

In the unsteady simulations a periodic behaviour in the monitored flow variables was seen. Figure 19 shows the pressures in some of the monitored points on the TMS vane.

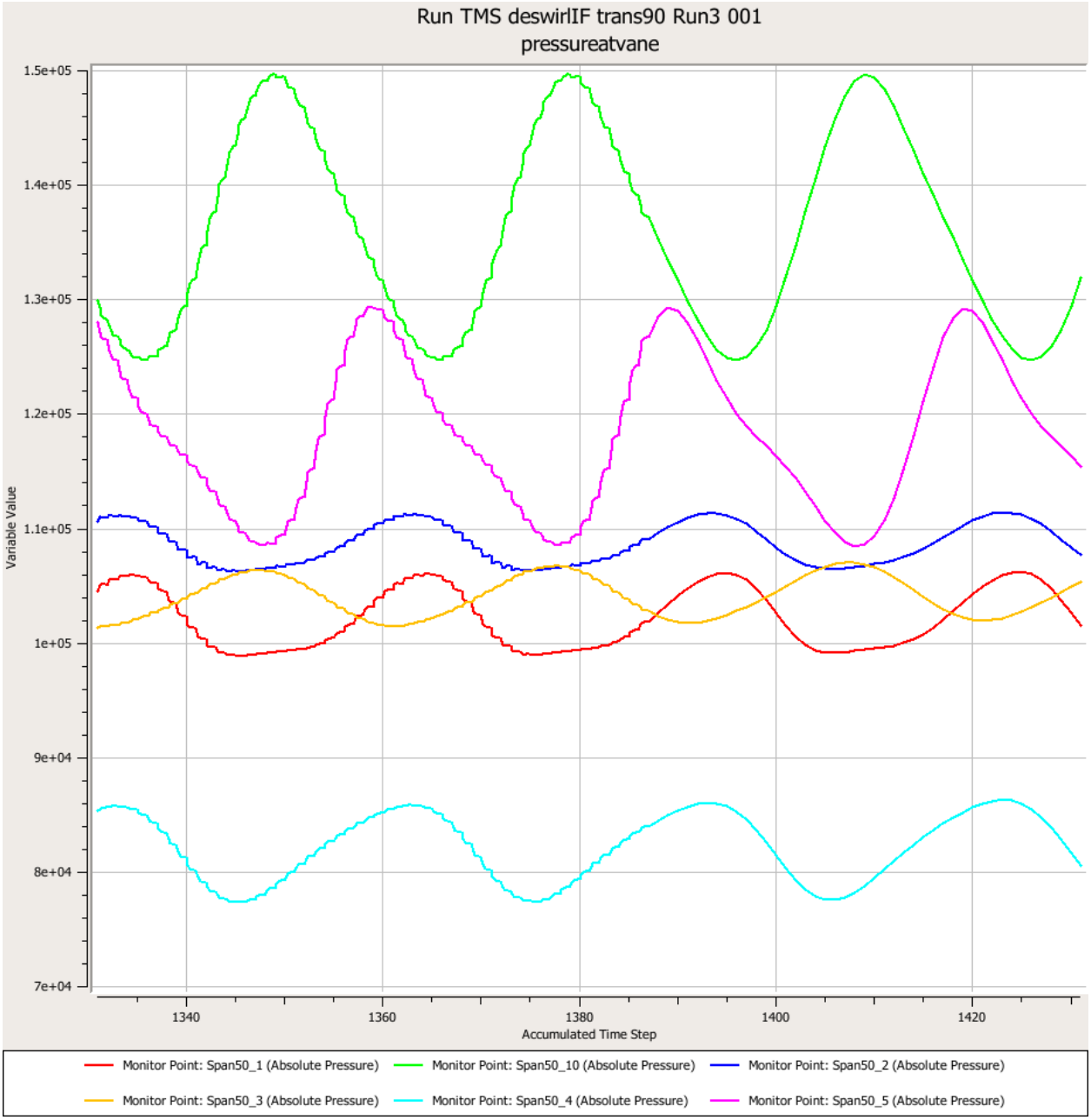

Figure 18: The periodic behaviour of the pressure at the TMS vane. The period of the fluctuations is 30 timesteps.

Figure 19 shows the time averaged Nusselt number distributions of the timestep intervals 919 to 948 and 1400 to 1429. The distributions were obtained with the 90 degree simulation. The difference between the distributions is small. The solution is therefore considered to be converged.

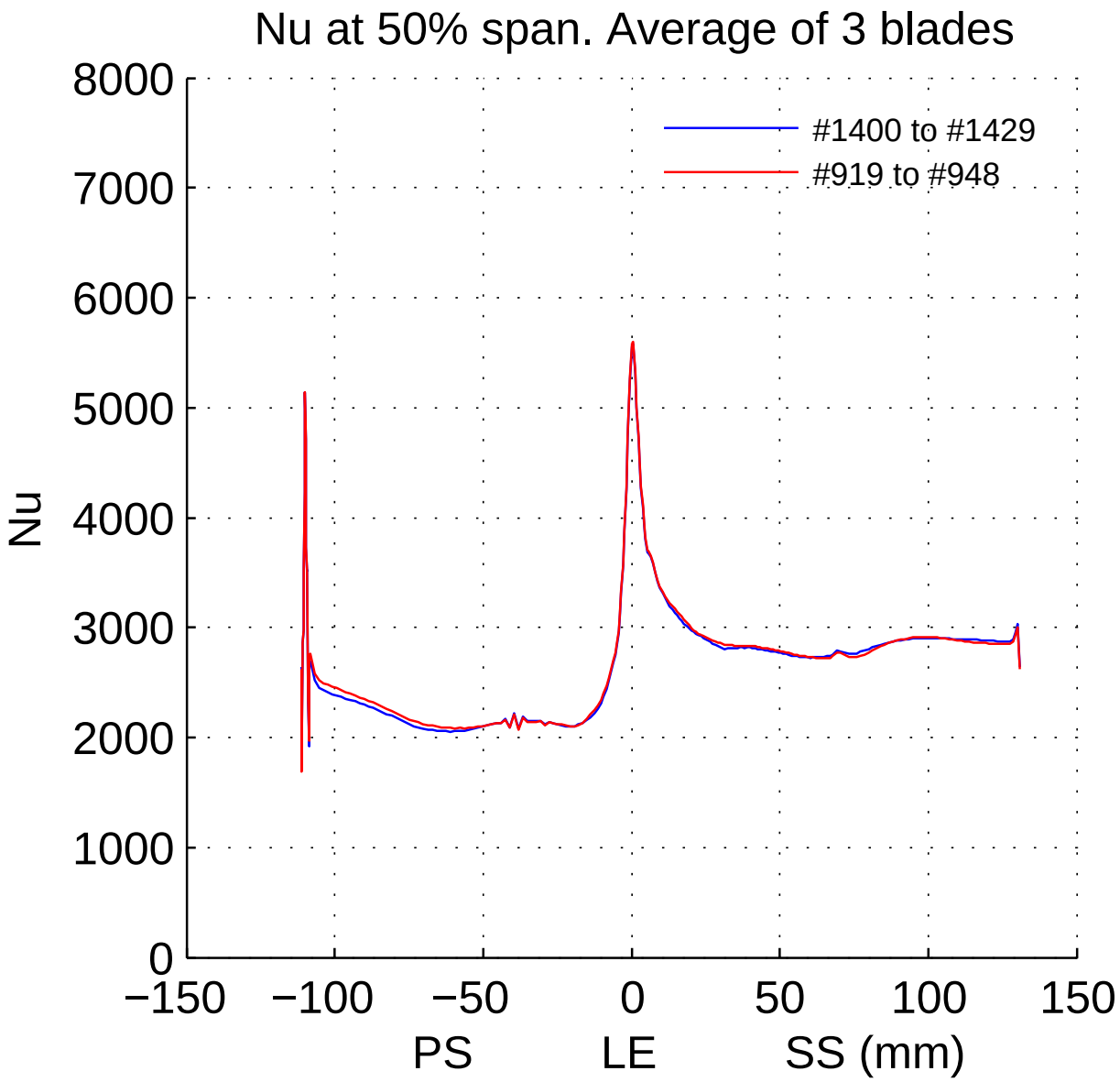

Figure 19: Time averaged Nusselt number distributions from different timestep intervals.

4.2 Heat Transfer

The Nusselt number distributions at 50% span obtained using the three different simulation methods are presented below in figure 20.

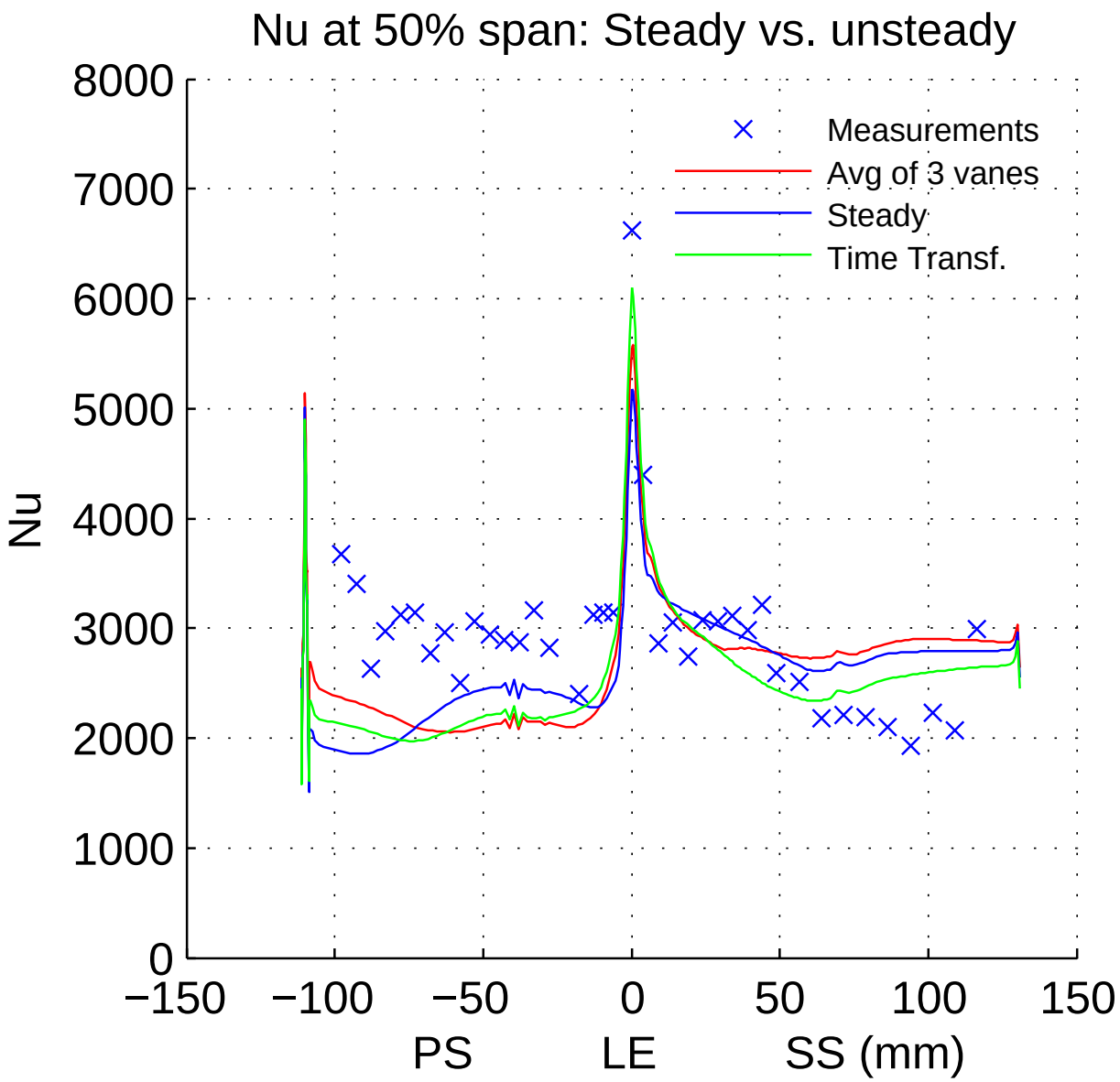

Figure 20: Results from the steady simulation, the 90 degree unsteady simulation and the Time Transformation simulation. *Nu* is plotted against the arc length of the curve shown in figure 16. PS: pressure side. LE: leading edge. SS: suction side. The unsteady results are time averaged. The measurements and the red curve show the average values of three adjacent vanes.

Figure 21 shows the Nusselt number distributions of adjacent vanes. CFD results from four vanes are included for comparing the first and fourth vane. The ratio between the number of stator vanes to TMS vanes is 32:24 = 4:3. There are eight '4:3-sectors' in the turbine. The disturbances felt by a TMS vane in one of these sectors are the same as those felt by a corresponding TMS vane in another sector. As can be seen in figure 21 the 4:3 ratio is reflected in the result as vane 1 and vane 4 have very similar Nusselt number distributions.

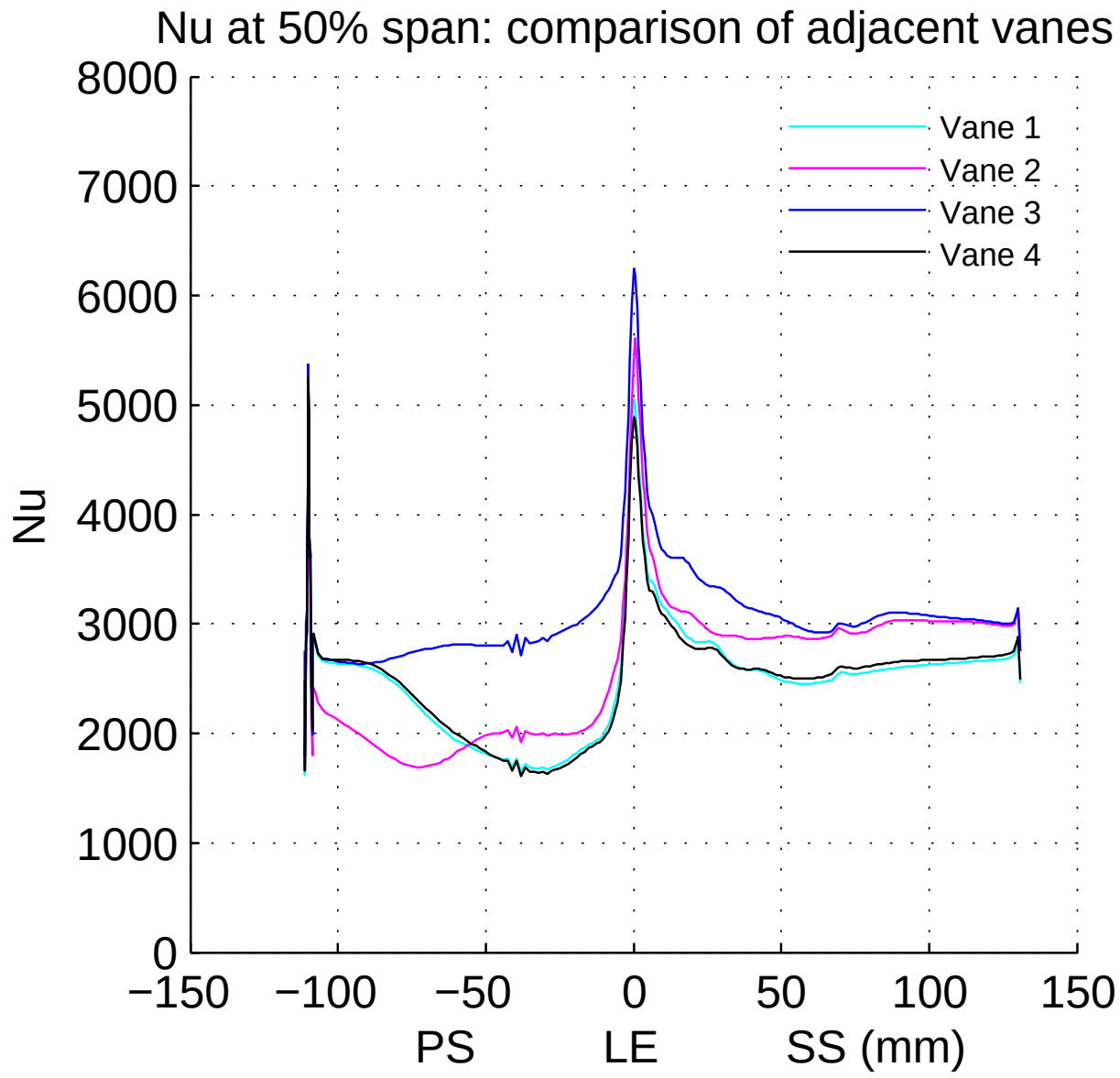

Figure 21: A comparison of adjacent vanes in the 90 degree transient simulation. Note that CFD results from four vanes are included.

Figure 22 shows how the Nusselt number distribution varies in time around the time averaged distribution. Timestep 15 is half a period from timestep 1.

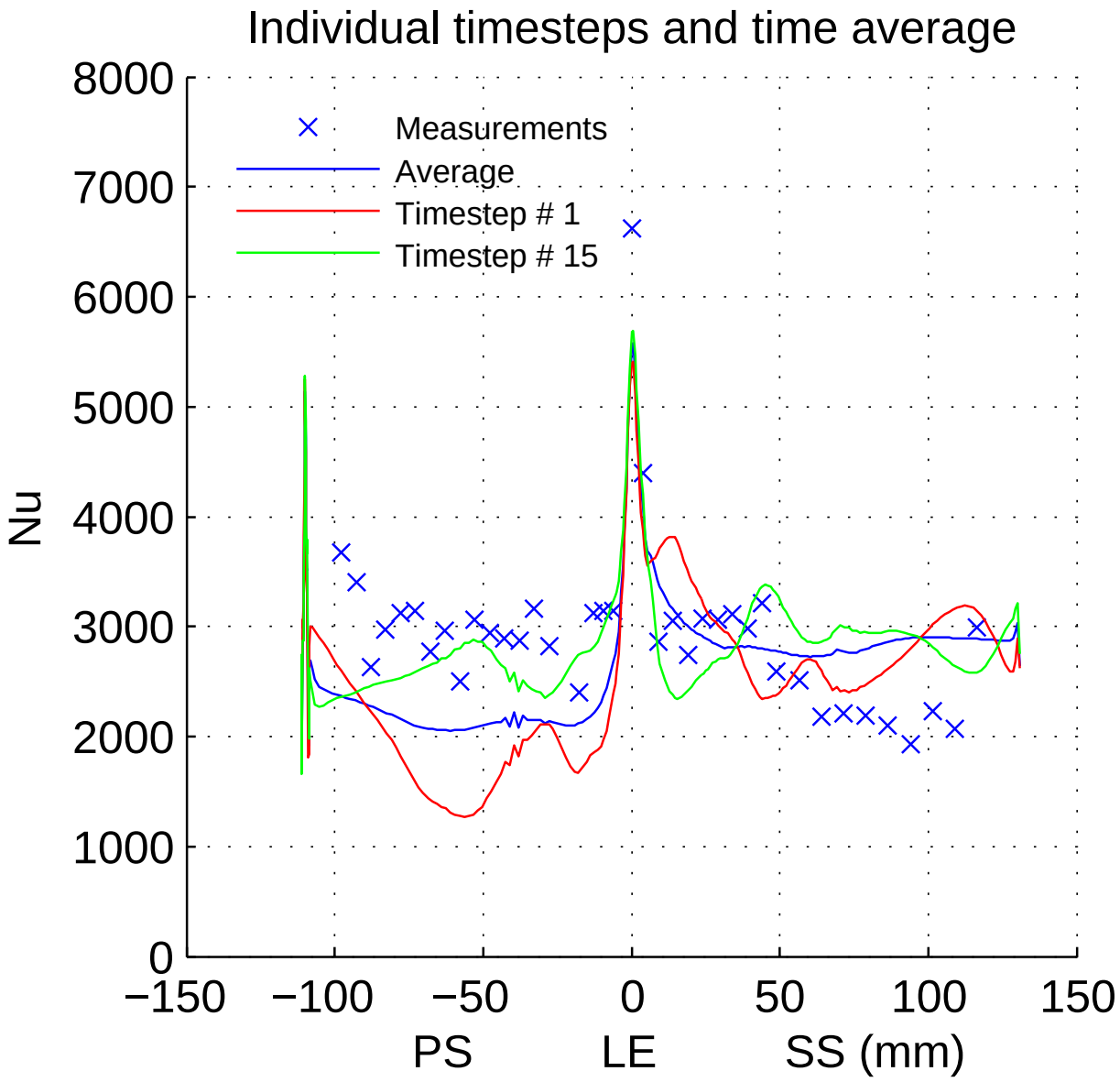

Figure 22: A comparison of the Nusselt number distribution from the 90 degree simulation at different timesteps and the time averaged distribution.

4.3 The dependence of results on mesh size, timestep and wall temperature.

Figure 23 shows that the Nusselt number distribution depends on the specified wall temperature. The wall temperature was changed from 300 K to 310 K and 400 K in steady simulations.

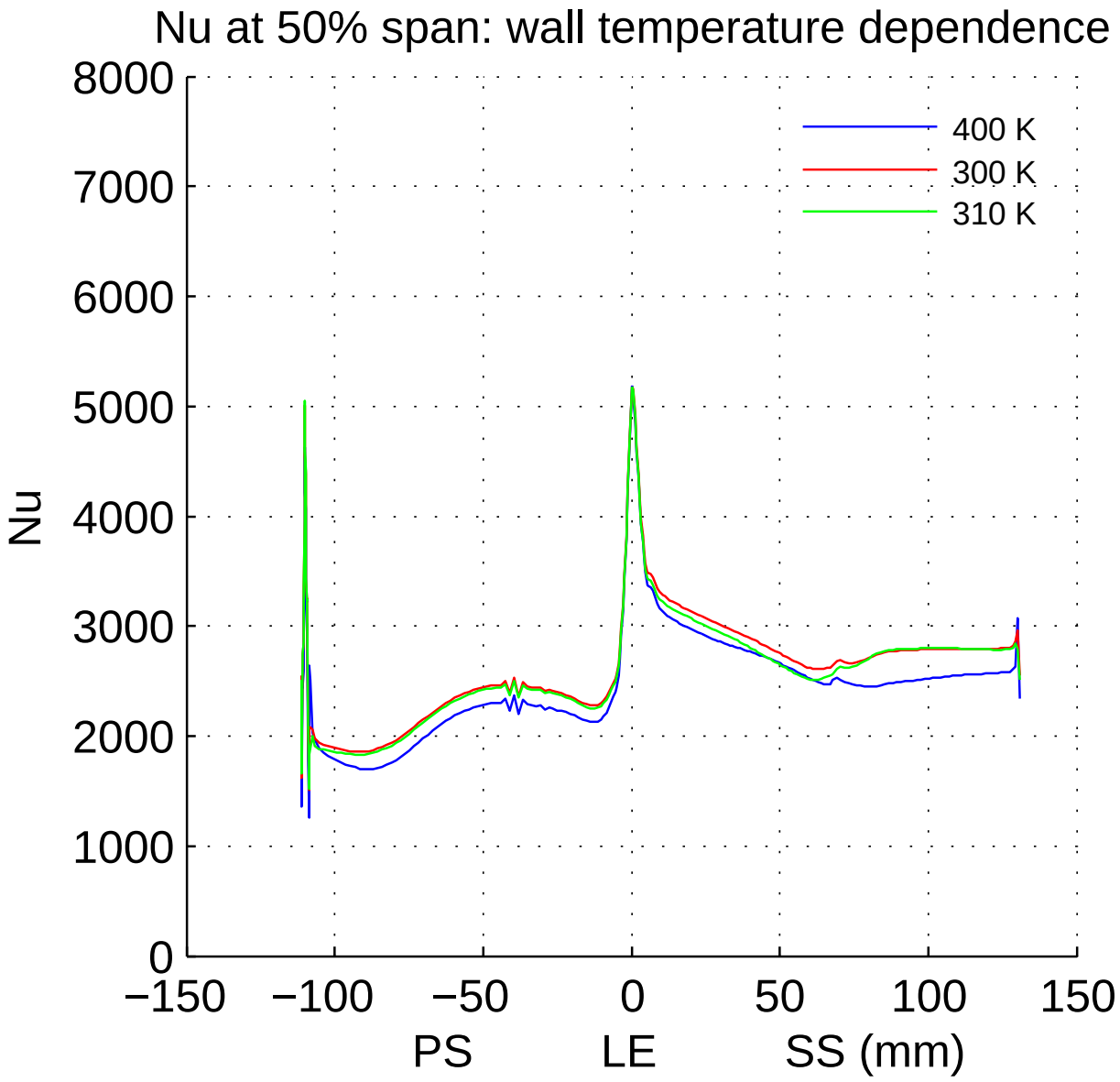

Figure 23: The effect of changing the wall temperature in the TMS domain.

Halving the timestep size did not affect the Nusselt number distribution significantly. In figure 24 the results from two Time Transformation simulations as well as the steady simulation are shown. The timesteps, 1/30 of the disturbance period, and the halved timestep give similar results.

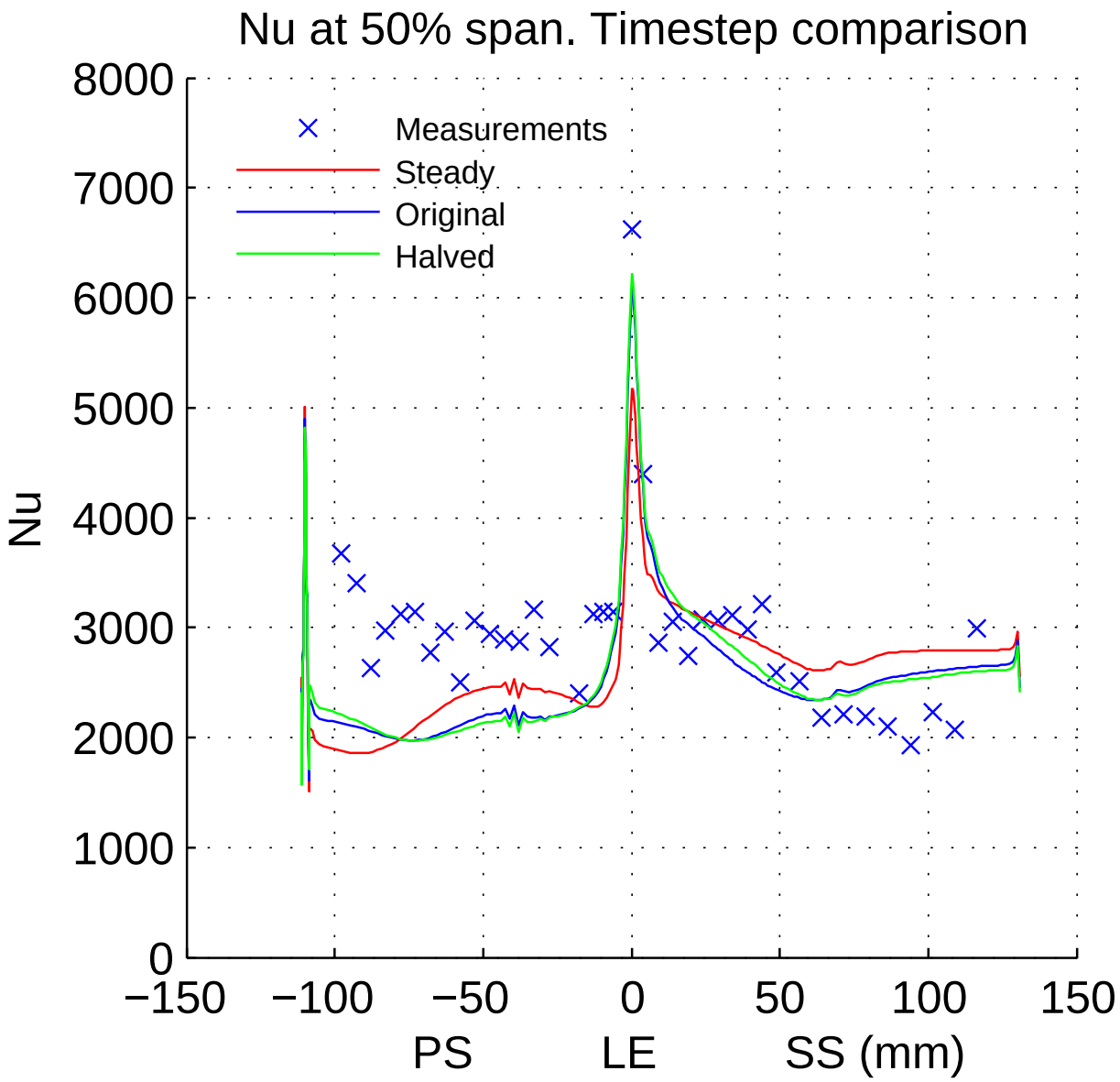

Figure 24: The effect of halving the timestep in the Time Transformation simulation.

Nusselt number distributions from steady simulations with refined TMS meshes are shown in figure 25. Differences between the original 2 million cell mesh and the refined meshes are noticable on the pressure side.

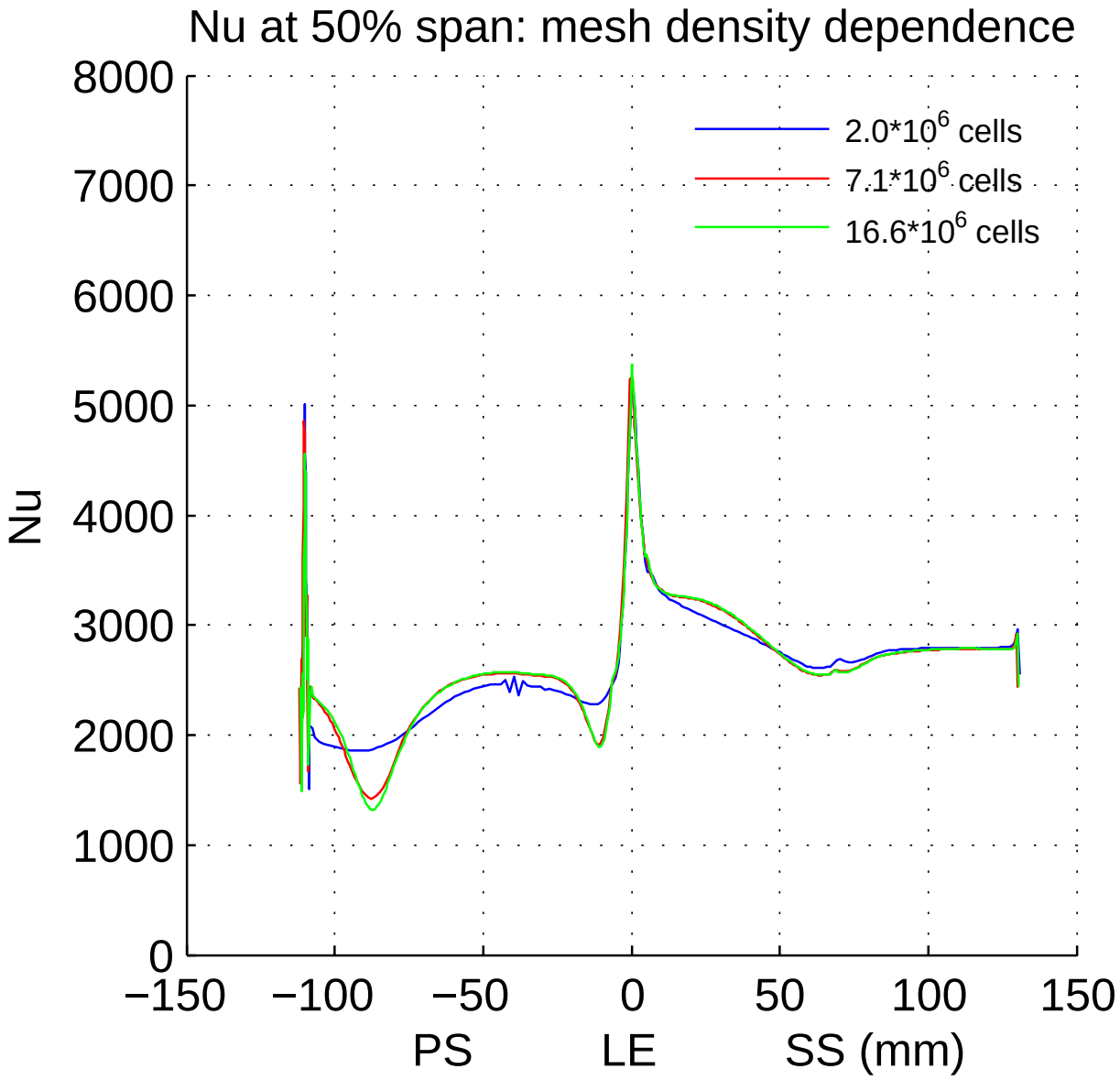

Figure 25: The effect of refining the TMS mesh.

Figure 26 reveals the difference between the wall heat flux predictions of the 2.0 million mesh and the 16.6 million mesh on the pressure side of the TMS vane.

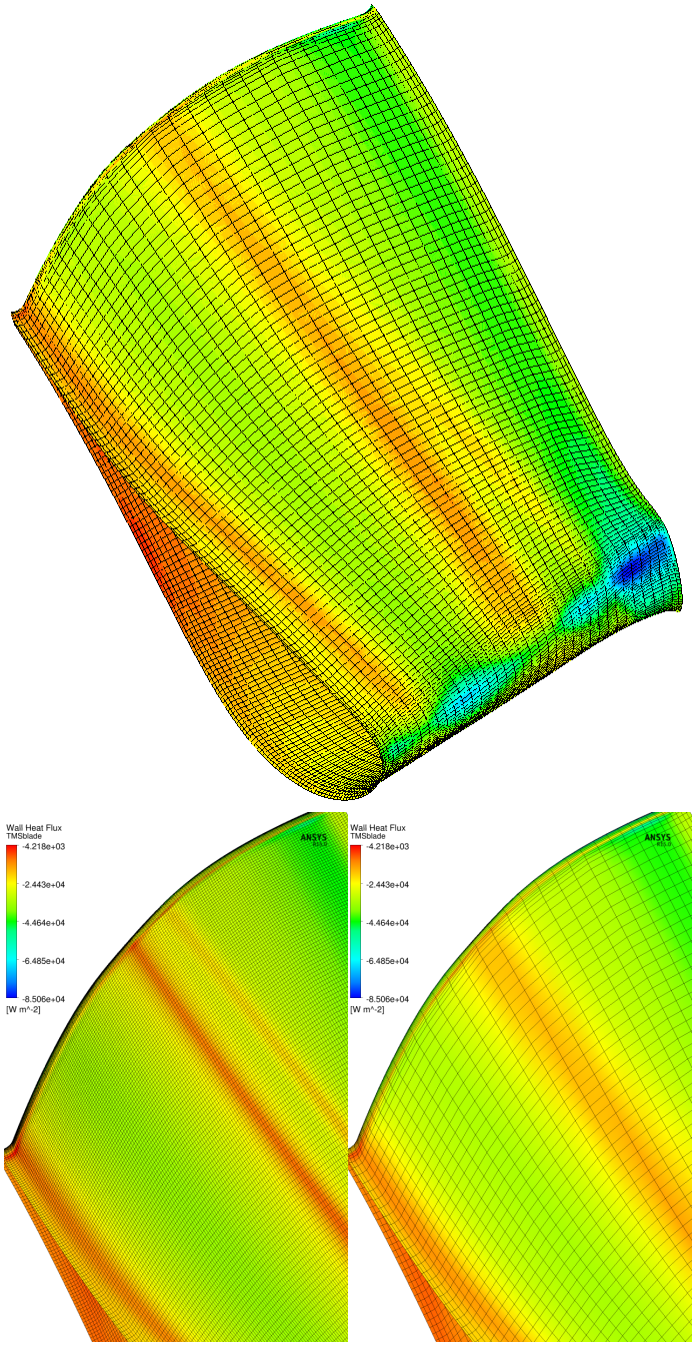

Figure 26: The wall heat flux predictions with the 2.0 million cells mesh and 16.6 million cells mesh. The upper figure shows the wall heat flux contour from the 2.0 million cells simulation on the pressure side of the TMS vane. The upper edge is the trailing edge and the lower edge is the leading edge. The lower figures show wall heat flux contours on the pressure side of the vane near the trailing edge from the 16.6 and 2.0 million cells simulation respectively.

Replacing the coarse stator and rotor meshes with the finer unmodified meshes had an effect on the Nusselt number distribution in steady simulations. This is clear from figure 27. The CFD result with fine stator and rotor meshes matches the measurements better on the leading part of the pressure side.

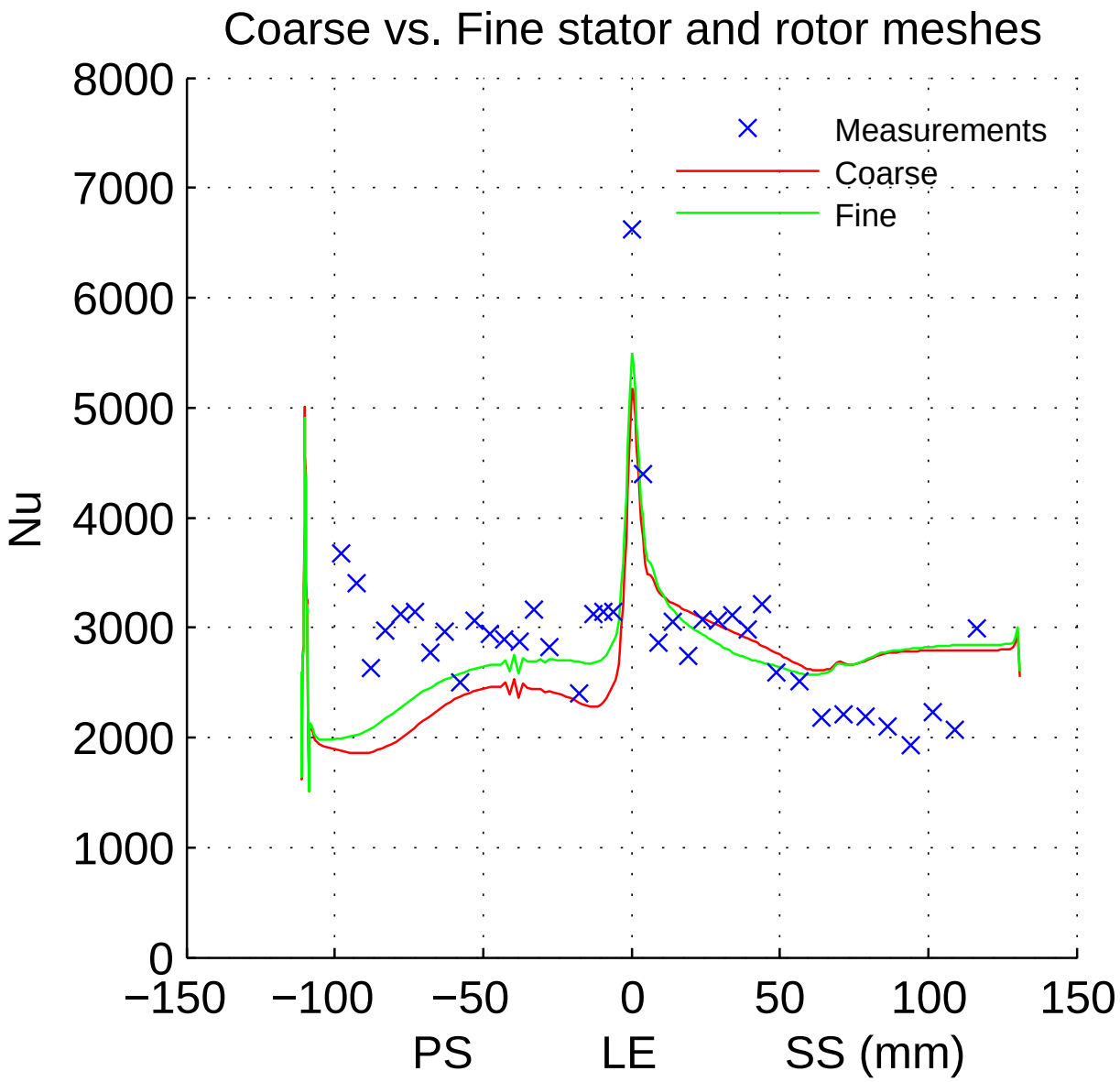

Figure 27: A comparison of steady results with coarse and fine stator and rotor meshes. The coarse stator mesh has 240,000 cells and the coarse rotor mesh has 960,000 cells. The finer meshes have 700,000 and 1,600,000 cells respectively.

Figure 28 shows pressure profiles at 50% span from the steady simulations with the three TMS mesh sizes discussed above as well as the result from a Time Transformation simulation. Experimental data from three adjacent vanes are also shown. The pressure profiles from the steady simulations appear to depend little on TMS mesh size. The shape of the Time Transformation pressure profile matches the shape of the measured pressure profile slightly better than it does in the steady simulations.

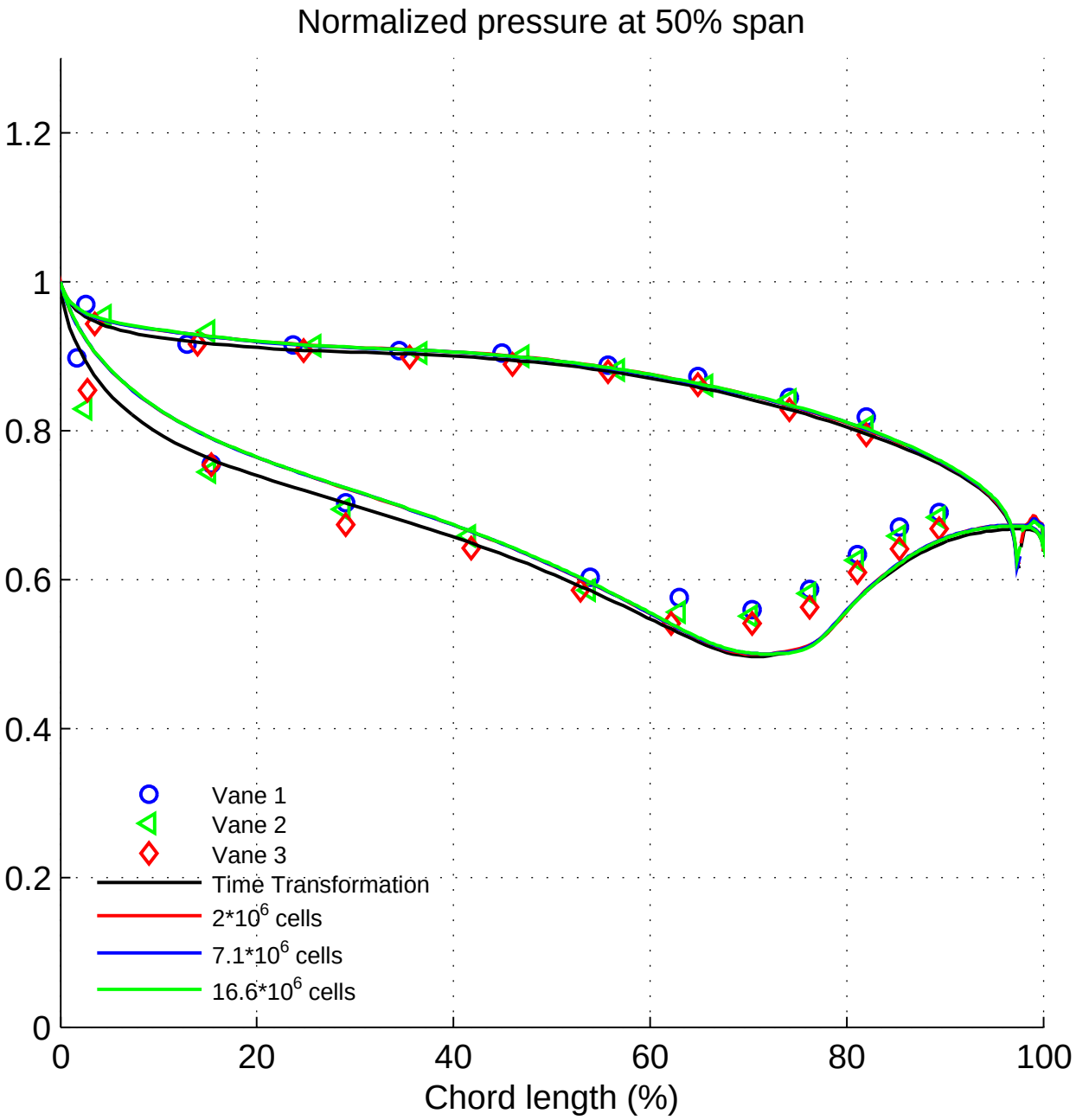

Figure 28: Normalized pressure profiles versus axial chord length. The measurements are from three adjacent vanes.

5 Discussion and further work

The results presented in the section above give a first indication of how the predictions of three simulation approaches in CFX compare with each other and with measurements.

The steady and unsteady results are almost identical in small intervals close to the leading edge and they all have similar peaks on the pressure side near the trailing edge. Elsewhere differences are more pronounced. In the immediate vicinity of the leading edge the unsteady simulations predict higher Nusselt numbers than the steady simulation. On the pressure side, approximately 40 mm from the leading edge, the Nusselt number distributions have an unsmooth behaviour. This is seen in the results of simulations in which the 2.0 million cells TMS mesh has been used. The reason for this unsmooth behaviour is not known. I does not appear to be caused by some quality deficiency in the TMS mesh. It might be related to how CFD Post extracts data from the results file.

Compared to the measurements the CFD predicts lower values of the Nusselt number on the pressure side and on the leading edge. The measurements do not show the same tendency for a sharp peak near the trailing edge on the pressure side as the CFD does. Rather, the Nusselt number increases gradually towards the trailing edge. It would be interesting to compare the CFD with measurements at the location where the CFD predicts a peak. Measurements have not been conducted at that location in the vicinity of the trailing edge. There is a better agreement between the CFD results and the measurements in the interval 10 to 50 mm from the leading edge on the suction side. The CFD simulations predict higher values of the Nusselt number on the suction side than on the pressure side. This is in some contrast to the measurements which are actually lower on the suction side compared to the pressure side beyond 50 mm from the leading edge.

The steady simulation predicts two minimas in the Nusselt number distribution at 50% span on the pressure side. Refining the TMS meshes tend to result in more distinct minimas but elsewhere the change in Nusselt number distribution is small. The aspect ratio of near-wall cells in heat transfer predictions might not be as important as the near-wall resolution and y^+. The difference between the results of the simulations with finer TMS meshes and the original TMS mesh might only be attributed to the higher near-wall and radial resolution and not to a lower aspect ratio since all three of these parameters have been changed and not only the aspect ratio. The use of finer stator and rotor meshes has a rather noticable effect on the pressure side of the TMS vane. It is clear that the results are not mesh-independent and they do not give a definite answer to the question of how well CFX can predict heat transfer in this turbine. A more rigorous mesh refinement study might produce results that match the measurements better. Although comparisons of the three analysis types can be made. The steady simulation is the computationally cheapest one and the result at 50% span is rather similar compared to the time averaged unsteady results. The Time Transformation method is a cheaper alternative to the 90 degree simulation. It would be feasible to use this method with boundary layer resolving stator and rotor meshes. The 90 degree simulation involves less modeling than the other two simulations and is expected to give more accurate

results and capture differences between vanes. In this simulation it was deemed necessary to use coarse meshes and wallfunctions in the stator and rotor domains which probably makes the results less accurate.

The adiabatic wall temperature was used as reference temperature for calculating the convection heat transfer coefficient in this project and for obtaining the heat transfer coefficent from the heat transfer measurements in the test rig. A disadvantage with this approach is that extra simulations with adiabatic walls must be carried out. This is not necessary if some bulk temperature is used instead. With the adiabatic wall temperature as reference temperature the Nusselt number distribution is expected to be independent of the specified wall temperature. However, figure 23 shows that there exists a temperature dependence. Using the obtained thermal conductivity distribution at 50% span for each specified wall temperature, instead of a constant value, does not give a temperature independent Nusselt number distribution either. The Nusselt number distribution close to the leading edge seems to be less dependent on the specified wall temperature.

Suggested further work includes more post processing of the results. Unsteady simulations, using a transient blade row model like the Time Transformation method, and steady simulations can be conducted without a need for using coarse meshes in parts of the domain. The effect from surface roughness on the heat transfer can be studied with models in CFX. In all simulations discussed above the boundary layers have been assumed fully turbulent. The effect of transition models on the results could be investigated.

References

[1] Rolls Royce plc, *The Jet Engine*, Rolls-Royce plc, 1996, pp. 1-51, p. 208.

[2] Kundu P.K., Cohen I.M. *Fluid Mechanics, Fourth Edition*, Academic Press, 2010, pp. 411-416.

[3] Johansson A.V., Wallin S., *Turbulence Lecture Notes*, KTH, 2012, pp.1-8.

[4] Incropera F.P., DeWitt D.P., Bergman T.L., Lavine A.S., *Fundamentals of Heat and Mass Transfer*, 6:th edition, Wiley, 2006.

[5] Pope S.B., *Turbulent Flows*, Cambridge University Press, 2011.

[6] ANSYS Inc., ANSYS 14.5 Theory Guide.

[7] ANSYS Inc., ANSYS 14.5 Modeling Guide.

[8] ANSYS Inc., ANSYS 14.5 Reference Guide.

[9] Tu J., Yeoh G.H., Liu C., *Computational Fluid Dynamics A Practical Approach*, first edition, Elsevier, 2008.

[10] Baskharone E.A., *Principles of Turbomachinery in Air-Breathing Engines*, first edition, Cambridge University Press, 2006.

[11] Figure 1: Source: http://commons.wikimedia.org/wiki/File:Jet_engine.svg. Author: Jeff Dahl. Published under the GNU Free Documentation License: http://www.gnu.org/copyleft/fdl.html.

[12] Figure 4: Source: http://commons.wikimedia.org/wiki/File: Laminar_boundary_layer_scheme.svg. The original file has been modified. Creator: Flanker. Published under the GNU Free Documentation License: http://www.gnu.org/copyleft/fdl.html.

[13] Figure 5: Source: http://commons.wikimedia.org/wiki/File:Boundarylayerschematic.svg. The original file has been modified. Creator: Dantor. Published under the GNU Free Documentation License: http://www.gnu.org/copyleft/fdl.html.

[14] Hirsch C., *Numerical Computation of Internal & External Flows*, second edition, Butterworth-Heinemann, 2007.

[15] Doorly J.E., Oldfield M.L.G., *The theory of advanced multi-layer thin film heat transfer gauges*, International Journal of Heat and Mass Transfer, Vol. 30, No. 6, pp. 1159-1168, 1987.

[16] Oldfield M.L.G., *Impulse Response Processing of Transient Heat Transfer Gauge Signals*, Journal of Turbomachinery, April 2008, Vol. 130 / 021023-1.

[17] Piccini E., *The development of a new heat transfer gauge for heat transfer facilites*, Master's thesis, University of Oxford, 1999.

Appendix

Steady simulation settings

2. Mesh Report

Table 2. Mesh Information for TMS_deswirlIF_003_001
Domain Nodes Elements
deswirl 308560 290433
Rotor 734280 702628
Stator 255308 242001
TMS 2096464 2045801
All Domains 3394612 3280863

3. Physics Report

Table 3. Domain Physics for TMS_deswirlIF_003_001
Domain - Deswirl
Type Fluid
Location FLUID 4
Materials
GKN Air Ideal Gas
    Fluid Definition Material Library
    Morphology Continuous Fluid
Settings
Buoyancy Model Non Buoyant
Domain Motion Stationary
Reference Pressure 0.0000e+00 [atm]
Heat Transfer Model Total Energy
    Include Viscous Work Term On
Turbulence Model SST
    Transitional Turbulence Fully Turbulent
Turbulent Wall Functions Automatic
    High Speed Model Off
Domain - Rotor
Type Fluid
Location FLUID 3
Materials
GKN Air Ideal Gas
    Fluid Definition Material Library
    Morphology Continuous Fluid
Settings
Buoyancy Model Non Buoyant
Domain Motion Rotating
    Angular Velocity 9.5000e+03 [rev min^-1]
    Axis Definition Coordinate Axis
    Rotation Axis Coord 0.1
Reference Pressure 0.0000e+00 [atm]
Heat Transfer Model Total Energy
    Include Viscous Work Term On
Turbulence Model SST
    Transitional Turbulence Fully Turbulent
Turbulent Wall Functions Automatic
    High Speed Model Off
Domain - Stator
Type Fluid
Location FLUID 2
Materials
GKN Air Ideal Gas
    Fluid Definition Material Library
    Morphology Continuous Fluid
Settings
Buoyancy Model Non Buoyant
Domain Motion Stationary
Reference Pressure 0.0000e+00 [atm]
Heat Transfer Model Total Energy
    Include Viscous Work Term On
Turbulence Model SST
    Transitional Turbulence Fully Turbulent
Turbulent Wall Functions Automatic
    High Speed Model Off
Domain - TMS
Type Fluid
Location FLUID
Materials
GKN Air Ideal Gas
    Fluid Definition Material Library
    Morphology Continuous Fluid
Settings
Buoyancy Model Non Buoyant
Domain Motion Stationary
Reference Pressure 0.0000e+00 [atm]
Heat Transfer Model Total Energy
    Include Viscous Work Term On
Turbulence Model SST
    Transitional Turbulence Fully Turbulent
Turbulent Wall Functions Automatic
    High Speed Model Off
Domain Interface - DeswirlPERINT
Boundary List1 DeswirlPERINT Side 1
Boundary List2 DeswirlPERINT Side 2
Interface Type Fluid Fluid
Settings
Interface Models Rotational Periodicity
    Axis Definition Coordinate Axis
    Rotation Axis Coord 0.1
Mesh Connection Direct
Domain Interface - Rotor TMS
Boundary List1 Rotor TMS Side 1
Boundary List2 Rotor TMS Side 2
Interface Type Fluid Fluid
Settings
Interface Models General Connection
    Frame Change Stage
    Downstream Velocity Constraint Stage Average Velocity
Pitch Change Specified Pitch Angles
    Pitch Angle Side1 6.0000e+00 [degree]
    Pitch Angle Side2 1.5000e+01 [degree]
Mesh Connection GGI
    Intersection Control Direct
Domain Interface - RotorPERINT
Boundary List1 RotorPERINT Side 1
Boundary List2 RotorPERINT Side 2
Interface Type Fluid Fluid
Settings
Interface Models Rotational Periodicity
    Axis Definition Coordinate Axis
    Rotation Axis Coord 0.1
Mesh Connection Direct
Domain Interface - Stator Rotor
Boundary List1 Stator Rotor Side 1
Boundary List2 Stator Rotor Side 2
Interface Type Fluid Fluid
Settings
Interface Models General Connection
    Frame Change Stage
    Downstream Velocity Constraint Stage Average Velocity
Pitch Change Specified Pitch Angles
    Pitch Angle Side1 1.1250e+01 [degree]
    Pitch Angle Side2 6.0000e+00 [degree]
Mesh Connection GGI
    Intersection Control Direct
Domain Interface - StatorPERINT
Boundary List1 StatorPERINT Side 1
Boundary List2 StatorPERINT Side 2
Interface Type Fluid Fluid
Settings
Interface Models Rotational Periodicity
    Axis Definition Coordinate Axis
    Rotation Axis Coord 0.1
Mesh Connection Direct
Domain Interface - TMS Deswirl
Boundary List1 TMS Deswirl Side 1
Boundary List2 TMS Deswirl Side 2
Interface Type Fluid Fluid
Settings
Interface Models General Connection
    Frame Change Stage
    Downstream Velocity Constraint Stage Average Velocity
Pitch Change Specified Pitch Angles
    Pitch Angle Side1 1.5000e+01 [degree]
    Pitch Angle Side2 7.5000e+00 [degree]
    Axis Definition Coordinate Axis
    Rotation Axis Coord 0.1
Mesh Connection GGI
    Intersection Control Direct
Domain Interface - TMSPERINT
Boundary List1 TMSPERINT Side 1
Boundary List2 TMSPERINT Side 2
Interface Type Fluid Fluid
Settings
Interface Models Rotational Periodicity
    Axis Definition Coordinate Axis
    Rotation Axis Coord 0.1
Mesh Connection Direct

Table 4. Boundary Physics for TMS_deswirlIF_003_001
Domain Boundaries
Deswirl Boundary - DeswirlPERINT Side 1
Type INTERFACE
Location PER1
Settings
Heat Transfer Conservative Interface Flux
Mass And Momentum Conservative Interface Flux
Turbulence Conservative Interface Flux
Boundary - DeswirlPERINT Side 2
Type INTERFACE

```
Location PER2
Settings
Heat Transfer Conservative Interface Flux
Mass And Momentum Conservative Interface Flux
Turbulence Conservative Interface Flux
Boundary - TMS Deswirl Side 2
Type INTERFACE
Location INLET 2
Settings
Heat Transfer Conservative Interface Flux
Mass And Momentum Conservative Interface Flux
Turbulence Conservative Interface Flux
Boundary - DeswirlOUTLET
Type OUTLET
Location OUTLET
Settings
Flow Regime Subsonic
Mass And Momentum Average Static Pressure
     Pressure Profile Blend  5.0000e-02
     Relative Pressure  1.2000e+02 [kPa]
Pressure Averaging Average Over Whole Outlet
Boundary - HUB_SHR_DESWIRL
Type WALL
Location "HUB, SHROUD, VANE"
Settings
Heat Transfer Fixed Temperature
     Fixed Temperature WallTemp
Mass And Momentum No Slip Wall
Wall Roughness Smooth Wall
Rotor Boundary - Rotor TMS Side 1
Type INTERFACE
Location CENTER OUTLET 2
Settings
Heat Transfer Conservative Interface Flux
Mass And Momentum Conservative Interface Flux
Turbulence Conservative Interface Flux
Boundary - RotorPERINT Side 1
Type INTERFACE
Location CENTER PER 1 2
Settings
Heat Transfer Conservative Interface Flux
Mass And Momentum Conservative Interface Flux
Turbulence Conservative Interface Flux
Boundary - RotorPERINT Side 2
Type INTERFACE
Location CENTER PER 2 2
Settings
Heat Transfer Conservative Interface Flux
Mass And Momentum Conservative Interface Flux
Turbulence Conservative Interface Flux
Boundary - Stator Rotor Side 2
Type INTERFACE
Location CENTER INLET 2
Settings
Heat Transfer Conservative Interface Flux
Mass And Momentum Conservative Interface Flux
Turbulence Conservative Interface Flux
Boundary - HUB_Counterrot
Type WALL
Location HUB COUNTERROT
Settings
Heat Transfer Fixed Temperature
     Fixed Temperature WallTemp
Mass And Momentum No Slip Wall
     Wall Velocity Counter Rotating Wall
Wall Roughness Smooth Wall
Boundary - HUB_ROTOR
Type WALL
Location HUB 3
Settings
Heat Transfer Fixed Temperature
     Fixed Temperature WallTemp
Mass And Momentum No Slip Wall
Wall Roughness Smooth Wall
Boundary - RotorBlade
Type WALL
Location FILLET HUB
Settings
Heat Transfer Fixed Temperature
     Fixed Temperature WallTemp
Mass And Momentum No Slip Wall
Wall Roughness Smooth Wall
Boundary - SHROUD
Type WALL
Location "CENTER SHROUD, BLADE TIP SHR"
Settings
Heat Transfer Fixed Temperature
     Fixed Temperature WallTemp
Mass And Momentum No Slip Wall
     Wall Velocity Counter Rotating Wall
Wall Roughness Smooth Wall
Stator Boundary - StatorInlet
Type INLET
Location CENTER INLET
Settings
Flow Direction Normal to Boundary Condition
Flow Regime Subsonic
Heat Transfer Total Temperature
     Total Temperature  4.4400e+02 [K]
Mass And Momentum Total Pressure
     Relative Pressure  4.6000e+00 [bar]
Turbulence Medium Intensity and Eddy Viscosity Ratio
Boundary - Stator Rotor Side 1
Type INTERFACE
Location CENTER OUTLET
Settings
Heat Transfer Conservative Interface Flux
Mass And Momentum Conservative Interface Flux
Turbulence Conservative Interface Flux
Boundary - StatorPERINT Side 1
Type INTERFACE
Location CENTER PER 1
Settings
Heat Transfer Conservative Interface Flux
Mass And Momentum Conservative Interface Flux
Turbulence Conservative Interface Flux
Boundary - StatorPERINT Side 2
Type INTERFACE
Location CENTER PER 2
Settings
Heat Transfer Conservative Interface Flux
Mass And Momentum Conservative Interface Flux
Turbulence Conservative Interface Flux
Boundary - StatorBlade
Type WALL
Location VANE 2
Settings
Heat Transfer Fixed Temperature
     Fixed Temperature WallTemp
Mass And Momentum No Slip Wall
Wall Roughness Smooth Wall
Boundary - StatorHub
Type WALL
Location HUB 2
Settings
Heat Transfer Fixed Temperature
     Fixed Temperature WallTemp
Mass And Momentum No Slip Wall
Wall Roughness Smooth Wall
Boundary - StatorShroud
Type WALL
Location SHROUD 2
Settings
Heat Transfer Fixed Temperature
     Fixed Temperature WallTemp
Mass And Momentum No Slip Wall
Wall Roughness Smooth Wall
TMS Boundary - Rotor TMS Side 2
Type INTERFACE
Location INLET
Settings
Heat Transfer Conservative Interface Flux
Mass And Momentum Conservative Interface Flux
Turbulence Conservative Interface Flux
Boundary - TMS Deswirl Side 1
Type INTERFACE
Location UPSTREAM_OUTLET
Settings
Heat Transfer Conservative Interface Flux
Mass And Momentum Conservative Interface Flux
Turbulence Conservative Interface Flux
Boundary - TMSPERINT Side 1
Type INTERFACE
Location FAM20
Settings
Heat Transfer Conservative Interface Flux
Mass And Momentum Conservative Interface Flux
Turbulence Conservative Interface Flux
Boundary - TMSPERINT Side 2
Type INTERFACE
Location FAM21
Settings
Heat Transfer Conservative Interface Flux
Mass And Momentum Conservative Interface Flux
Turbulence Conservative Interface Flux
Boundary - TMSblade
Type WALL
Location BLADE_FILLETS
Settings
Heat Transfer Fixed Temperature
     Fixed Temperature WallTemp
Mass And Momentum No Slip Wall
Wall Roughness Smooth Wall
Boundary - TMShub
```

```
Type WALL
Location HUBFILLET
Settings
Heat Transfer Fixed Temperature
     Fixed Temperature WallTemp
Mass And Momentum No Slip Wall
Wall Roughness Smooth Wall
Boundary - TMSshroud
Type WALL
Location SHROUDFILLET
Settings
Heat Transfer Fixed Temperature
     Fixed Temperature WallTemp
Mass And Momentum No Slip Wall
Wall Roughness Smooth Wall
4. User Data
```

Time Transformation simulation settings

```
1. Mesh Report

Table 1.  Mesh Information for TimeTransformationSteady_001
Domain Nodes Elements
Deswirl 308560 290433
Rotor 2182740 2107884
Stator 506924 484002
TMS 2096464 2045801
All Domains 5094688 4928120


2. Physics Report

Table 2.  Domain Physics for TimeTransformationSteady_001
Domain - Deswirl
Type Fluid
Location FLUID 4
Materials
GKN Air Ideal Gas
     Fluid Definition Material Library
     Morphology Continuous Fluid
Settings
Buoyancy Model Non Buoyant
Domain Motion Stationary
Reference Pressure  0.0000e+00 [atm]
Heat Transfer Model Total Energy
     Include Viscous Work Term On
Turbulence Model SST
     Transitional Turbulence Fully Turbulent
Turbulent Wall Functions Automatic
     High Speed Model Off
Domain - Rotor
Type Fluid
Location "FLUID 3, FLUID 3 2, FLUID 3 3"
Materials
GKN Air Ideal Gas
     Fluid Definition Material Library
     Morphology Continuous Fluid
Settings
Buoyancy Model Non Buoyant
Domain Motion Rotating
     Angular Velocity  9.5000e+03 [rev min^-1]
     Axis Definition Coordinate Axis
     Rotation Axis Coord 0.1
Reference Pressure  0.0000e+00 [atm]
Heat Transfer Model Total Energy
     Include Viscous Work Term On
Turbulence Model SST
     Transitional Turbulence Fully Turbulent
Turbulent Wall Functions Automatic
     High Speed Model Off
Domain - Stator
Type Fluid
Location "FLUID 2, FLUID 2 2"
Materials
GKN Air Ideal Gas
     Fluid Definition Material Library
     Morphology Continuous Fluid
Settings
Buoyancy Model Non Buoyant
Domain Motion Stationary
Reference Pressure  0.0000e+00 [atm]
Heat Transfer Model Total Energy
     Include Viscous Work Term On
Turbulence Model SST
     Transitional Turbulence Fully Turbulent
Turbulent Wall Functions Automatic
     High Speed Model Off
Domain - TMS
Type Fluid
Location FLUID
Materials
GKN Air Ideal Gas
     Fluid Definition Material Library
     Morphology Continuous Fluid
Settings
Buoyancy Model Non Buoyant
Domain Motion Stationary
Reference Pressure  0.0000e+00 [atm]
Heat Transfer Model Total Energy
     Include Viscous Work Term On
Turbulence Model SST
     Transitional Turbulence Fully Turbulent
Turbulent Wall Functions Automatic
     High Speed Model Off
Domain Interface - DeswirlPERINT
Boundary List1 DeswirlPERINT Side 1
Boundary List2 DeswirlPERINT Side 2
Interface Type Fluid Fluid
Settings
Interface Models Rotational Periodicity
     Axis Definition Coordinate Axis
     Rotation Axis Coord 0.1
Mesh Connection Direct
Domain Interface - Rotor TMS
Boundary List1 Rotor TMS Side 1
Boundary List2 Rotor TMS Side 2
Interface Type Fluid Fluid
Settings
Interface Models General Connection
     Frame Change Stage
     Downstream Velocity Constraint Stage Average Velocity
Pitch Change Specified Pitch Angles
     Pitch Angle Side1  1.8000e+01 [degree]
     Pitch Angle Side2  1.5000e+01 [degree]
Mesh Connection GGI
     Intersection Control Direct
Domain Interface - RotorPERINT
Boundary List1 RotorPERINT Side 1
Boundary List2 RotorPERINT Side 2
Interface Type Fluid Fluid
Settings
Interface Models Rotational Periodicity
     Axis Definition Coordinate Axis
     Rotation Axis Coord 0.1
Mesh Connection Direct
Domain Interface - Stator Rotor
Boundary List1 Stator Rotor Side 1
Boundary List2 Stator Rotor Side 2
Interface Type Fluid Fluid
Settings
Interface Models General Connection
     Frame Change Stage
     Downstream Velocity Constraint Stage Average Velocity
Pitch Change Specified Pitch Angles
     Pitch Angle Side1  2.2500e+01 [degree]
     Pitch Angle Side2  1.8000e+01 [degree]
Mesh Connection GGI
     Intersection Control Direct
Domain Interface - StatorPERINT
Boundary List1 StatorPERINT Side 1
Boundary List2 StatorPERINT Side 2
Interface Type Fluid Fluid
Settings
Interface Models Rotational Periodicity
     Axis Definition Coordinate Axis
     Rotation Axis Coord 0.1
Mesh Connection Direct
Domain Interface - TMS Deswirl
Boundary List1 TMS Deswirl Side 1
Boundary List2 TMS Deswirl Side 2
Interface Type Fluid Fluid
Settings
Interface Models General Connection
     Frame Change Stage
     Downstream Velocity Constraint Stage Average Velocity
Pitch Change Specified Pitch Angles
     Pitch Angle Side1  1.5000e+01 [degree]
     Pitch Angle Side2  7.5000e+00 [degree]
     Axis Definition Coordinate Axis
     Rotation Axis Coord 0.1
Mesh Connection GGI
     Intersection Control Direct
Domain Interface - TMSPERINT
Boundary List1 TMSPERINT Side 1
Boundary List2 TMSPERINT Side 2
Interface Type Fluid Fluid
```

```
Settings
Interface Models Rotational Periodicity
     Axis Definition Coordinate Axis
     Rotation Axis Coord 0.1
Mesh Connection Direct


Table 3.  Boundary Physics for TimeTransformationSteady_001
Domain Boundaries
Deswirl Boundary - DeswirlPERINT Side 1
Type INTERFACE
Location PER1
Settings
Heat Transfer Conservative Interface Flux
Mass And Momentum Conservative Interface Flux
Turbulence Conservative Interface Flux
Boundary - DeswirlPERINT Side 2
Type INTERFACE
Location PER2
Settings
Heat Transfer Conservative Interface Flux
Mass And Momentum Conservative Interface Flux
Turbulence Conservative Interface Flux
Boundary - TMS Deswirl Side 2
Type INTERFACE
Location INLET 2
Settings
Heat Transfer Conservative Interface Flux
Mass And Momentum Conservative Interface Flux
Turbulence Conservative Interface Flux
Boundary - DeswirlOUTLET
Type OUTLET
Location OUTLET
Settings
Flow Regime Subsonic
Mass And Momentum Average Static Pressure
     Pressure Profile Blend  5.0000e-02
     Relative Pressure  1.2000e+02 [kPa]
Pressure Averaging Average Over Whole Outlet
Boundary - HUB_SHR_DESWIRL
Type WALL
Location "HUB, SHROUD, VANE"
Settings
Heat Transfer Fixed Temperature
     Fixed Temperature WallTemp
Mass And Momentum No Slip Wall
Wall Roughness Smooth Wall
Rotor Boundary - Rotor TMS Side 1
Type INTERFACE
Location "CENTER OUTLET 2, CENTER OUTLET 2 2, CENTER OUTLET 2 3"
Settings
Heat Transfer Conservative Interface Flux
Mass And Momentum Conservative Interface Flux
Turbulence Conservative Interface Flux
Boundary - RotorPERINT Side 1
Type INTERFACE
Location CENTER PER 1 2
Settings
Heat Transfer Conservative Interface Flux
Mass And Momentum Conservative Interface Flux
Turbulence Conservative Interface Flux
Boundary - RotorPERINT Side 2
Type INTERFACE
Location CENTER PER 2 2 3
Settings
Heat Transfer Conservative Interface Flux
Mass And Momentum Conservative Interface Flux
Turbulence Conservative Interface Flux
Boundary - Stator Rotor Side 2
Type INTERFACE
Location "CENTER INLET 2, CENTER INLET 2 2, CENTER INLET 2 3"
Settings
Heat Transfer Conservative Interface Flux
Mass And Momentum Conservative Interface Flux
Turbulence Conservative Interface Flux
Boundary - HUB_Counterrot
Type WALL
Location "HUB COUNTERROT, HUB COUNTERROT 2, HUB COUNTERROT 3"
Settings
Heat Transfer Fixed Temperature
     Fixed Temperature WallTemp
Mass And Momentum No Slip Wall
     Wall Velocity Counter Rotating Wall
Wall Roughness Smooth Wall
Boundary - HUB_ROTOR
Type WALL
Location "HUB 3, HUB 3 2, HUB 3 3"
Settings
Heat Transfer Fixed Temperature
     Fixed Temperature WallTemp
Mass And Momentum No Slip Wall
Wall Roughness Smooth Wall
Boundary - RotorBlade
Type WALL
Location "FILLET HUB, FILLET HUB 2, FILLET HUB 3"
Settings
Heat Transfer Fixed Temperature
     Fixed Temperature WallTemp
Mass And Momentum No Slip Wall
Wall Roughness Smooth Wall
Boundary - SHROUD
Type WALL
Location "CENTER SHROUD, BLADE TIP SHR, BLADE TIP SHR 2,
 BLADE TIP SHR 3, CENTER SHROUD 2, CENTER SHROUD 3"
Settings
Heat Transfer Fixed Temperature
     Fixed Temperature WallTemp
Mass And Momentum No Slip Wall
     Wall Velocity Counter Rotating Wall
Wall Roughness Smooth Wall
Stator Boundary - StatorInlet
Type INLET
Location "CENTER INLET, CENTER INLET 3"
Settings
Flow Direction Normal to Boundary Condition
Flow Regime Subsonic
Heat Transfer Total Temperature
     Total Temperature  4.4400e+02 [K]
Mass And Momentum Total Pressure
     Relative Pressure  4.6000e+00 [bar]
Turbulence Medium Intensity and Eddy Viscosity Ratio
Boundary - Stator Rotor Side 1
Type INTERFACE
Location "CENTER OUTLET, CENTER OUTLET 3"
Settings
Heat Transfer Conservative Interface Flux
Mass And Momentum Conservative Interface Flux
Turbulence Conservative Interface Flux
Boundary - StatorPERINT Side 1
Type INTERFACE
Location CENTER PER 1 3
Settings
Heat Transfer Conservative Interface Flux
Mass And Momentum Conservative Interface Flux
Turbulence Conservative Interface Flux
Boundary - StatorPERINT Side 2
Type INTERFACE
Location CENTER PER 2
Settings
Heat Transfer Conservative Interface Flux
Mass And Momentum Conservative Interface Flux
Turbulence Conservative Interface Flux
Boundary - StatorBlade
Type WALL
Location "VANE 2, VANE 2 2"
Settings
Heat Transfer Fixed Temperature
     Fixed Temperature WallTemp
Mass And Momentum No Slip Wall
Wall Roughness Smooth Wall
Boundary - StatorHub
Type WALL
Location "HUB 2, HUB 2 2"
Settings
Heat Transfer Fixed Temperature
     Fixed Temperature WallTemp
Mass And Momentum No Slip Wall
Wall Roughness Smooth Wall
Boundary - StatorShroud
Type WALL
Location "SHROUD 2, SHROUD 2 2"
Settings
Heat Transfer Fixed Temperature
     Fixed Temperature WallTemp
Mass And Momentum No Slip Wall
Wall Roughness Smooth Wall
TMS Boundary - Rotor TMS Side 2
Type INTERFACE
Location INLET
Settings
Heat Transfer Conservative Interface Flux
Mass And Momentum Conservative Interface Flux
Turbulence Conservative Interface Flux
Boundary - TMS Deswirl Side 1
Type INTERFACE
Location UPSTREAM_OUTLET
Settings
Heat Transfer Conservative Interface Flux
Mass And Momentum Conservative Interface Flux
Turbulence Conservative Interface Flux
Boundary - TMSPERINT Side 1
Type INTERFACE
Location FAM20
Settings
```

```
Heat Transfer Conservative Interface Flux
Mass And Momentum Conservative Interface Flux
Turbulence Conservative Interface Flux
Boundary - TMSPERINT Side 2
Type INTERFACE
Location FAM21
Settings
Heat Transfer Conservative Interface Flux
Mass And Momentum Conservative Interface Flux
Turbulence Conservative Interface Flux
Boundary - TMSblade
Type WALL
Location BLADE_FILLETS
Settings
Heat Transfer Fixed Temperature
     Fixed Temperature WallTemp
Mass And Momentum No Slip Wall
Wall Roughness Smooth Wall
Boundary - TMShub
Type WALL
Location HUBFILLET
Settings
Heat Transfer Fixed Temperature
     Fixed Temperature WallTemp
Mass And Momentum No Slip Wall
Wall Roughness Smooth Wall
Boundary - TMSshroud
Type WALL
Location SHROUDFILLET
Settings
Heat Transfer Fixed Temperature
     Fixed Temperature WallTemp
Mass And Momentum No Slip Wall
Wall Roughness Smooth Wall
```

90 degree simulation settings

```
1. Mesh Report

Table 1.  Mesh Information for TMS_deswirlIF_trans90_run2_007
Domain Nodes Elements
Deswirl 308560 290433
Rotor 10873500 10539420
Stator 2016620 1936008
TMS 12485704 12274806
All Domains 25684384 25040667


2. Physics Report

Table 2.  Domain Physics for TMS_deswirlIF_trans90_run2_007
Domain - Deswirl
Type Fluid
Location FLUID 4
Materials
GKN Air Ideal Gas
     Fluid Definition Material Library
     Morphology Continuous Fluid
Settings
Buoyancy Model Non Buoyant
Domain Motion Stationary
Reference Pressure  0.0000e+00 [atm]
Heat Transfer Model Total Energy
     Include Viscous Work Term On
Turbulence Model SST
     Transitional Turbulence Fully Turbulent
Turbulent Wall Functions Automatic
     High Speed Model Off
Domain - Rotor
Type Fluid
Location "FLUID 3, FLUID 3 10, FLUID 3 11, FLUID 3 12,
 FLUID 3 13, FLUID 3 14, FLUID 3 15, FLUID 3 2,
FLUID 3 3, FLUID 3 4, FLUID 3 5, FLUID 3 6,
 FLUID 3 7, FLUID 3 8, FLUID 3 9"
Materials
GKN Air Ideal Gas
     Fluid Definition Material Library
     Morphology Continuous Fluid
Settings
Buoyancy Model Non Buoyant
Domain Motion Rotating
     Angular Velocity  9.5000e+03 [rev min^-1]
     Axis Definition Coordinate Axis
     Rotation Axis Coord 0.1
Reference Pressure  0.0000e+00 [atm]
Heat Transfer Model Total Energy
     Include Viscous Work Term On
Turbulence Model SST
     Transitional Turbulence Fully Turbulent
Turbulent Wall Functions Automatic
     High Speed Model Off
Domain - Stator
Type Fluid
Location "FLUID 2, FLUID 2 2, FLUID 2 3, FLUID 2 4,
FLUID 2 5, FLUID 2 6, FLUID 2 7, FLUID 2 8"
Materials
GKN Air Ideal Gas
     Fluid Definition Material Library
     Morphology Continuous Fluid
Settings
Buoyancy Model Non Buoyant
Domain Motion Stationary
Reference Pressure  0.0000e+00 [atm]
Heat Transfer Model Total Energy
     Include Viscous Work Term On
Turbulence Model SST
     Transitional Turbulence Fully Turbulent
Turbulent Wall Functions Automatic
     High Speed Model Off
Domain - TMS
Type Fluid
Location "FLUID 5, FLUID 6, FLUID 7, FLUID 8, FLUID 9, FLUID"
Materials
GKN Air Ideal Gas
     Fluid Definition Material Library
     Morphology Continuous Fluid
Settings
Buoyancy Model Non Buoyant
Domain Motion Stationary
Reference Pressure  0.0000e+00 [atm]
Heat Transfer Model Total Energy
     Include Viscous Work Term On
Turbulence Model SST
     Transitional Turbulence Fully Turbulent
Turbulent Wall Functions Automatic
     High Speed Model Off
Domain Interface - DeswirlPERINT
Boundary List1 DeswirlPERINT Side 1
Boundary List2 DeswirlPERINT Side 2
Interface Type Fluid Fluid
Settings
Interface Models Rotational Periodicity
     Axis Definition Coordinate Axis
     Rotation Axis Coord 0.1
Mesh Connection Direct
Domain Interface - Rotor TMS
Boundary List1 Rotor TMS Side 1
Boundary List2 Rotor TMS Side 2
Interface Type Fluid Fluid
Settings
Interface Models General Connection
     Frame Change Transient Rotor Stator
Mass And Momentum Conservative Interface Flux
Pitch Change Specified Pitch Angles
     Pitch Angle Side1  9.0000e+01 [degree]
     Pitch Angle Side2  9.0000e+01 [degree]
Mesh Connection GGI
     Intersection Control Direct
Domain Interface - RotorPERINT
Boundary List1 RotorPERINT Side 1
Boundary List2 RotorPERINT Side 2
Interface Type Fluid Fluid
Settings
Interface Models Rotational Periodicity
     Axis Definition Coordinate Axis
     Rotation Axis Coord 0.1
Mesh Connection Direct
Domain Interface - Stator Rotor
Boundary List1 Stator Rotor Side 1
Boundary List2 Stator Rotor Side 2
Interface Type Fluid Fluid
Settings
Interface Models General Connection
     Frame Change Transient Rotor Stator
Mass And Momentum Conservative Interface Flux
Pitch Change Specified Pitch Angles
     Pitch Angle Side1  9.0000e+01 [degree]
     Pitch Angle Side2  9.0000e+01 [degree]
Mesh Connection GGI
     Intersection Control Direct
Domain Interface - StatorPERINT
Boundary List1 StatorPERINT Side 1
Boundary List2 StatorPERINT Side 2
Interface Type Fluid Fluid
Settings
Interface Models Rotational Periodicity
     Axis Definition Coordinate Axis
     Rotation Axis Coord 0.1
```

```
Mesh Connection Direct
Domain Interface - TMS Deswirl
Boundary List1 TMS Deswirl Side 1
Boundary List2 TMS Deswirl Side 2
Interface Type Fluid Fluid
Settings
Interface Models General Connection
     Frame Change Stage
     Downstream Velocity Constraint Stage Average Velocity
Pitch Change Specified Pitch Angles
     Pitch Angle Side1  9.0000e+01 [degree]
     Pitch Angle Side2  7.5000e+00 [degree]
     Axis Definition Coordinate Axis
     Rotation Axis Coord 0.1
Mesh Connection GGI
     Intersection Control Direct
Domain Interface - TMSPERINT
Boundary List1 TMSPERINT Side 1
Boundary List2 TMSPERINT Side 2
Interface Type Fluid Fluid
Settings
Interface Models Rotational Periodicity
     Axis Definition Coordinate Axis
     Rotation Axis Coord 0.1
Mesh Connection Direct


Table 3.  Boundary Physics for TMS_deswirlIF_trans90_run2_007
Domain Boundaries
Deswirl Boundary - DeswirlPERINT Side 1
Type INTERFACE
Location PER1
Settings
Heat Transfer Conservative Interface Flux
Mass And Momentum Conservative Interface Flux
Turbulence Conservative Interface Flux
Boundary - DeswirlPERINT Side 2
Type INTERFACE
Location PER2
Settings
Heat Transfer Conservative Interface Flux
Mass And Momentum Conservative Interface Flux
Turbulence Conservative Interface Flux
Boundary - TMS Deswirl Side 2
Type INTERFACE
Location INLET 2
Settings
Heat Transfer Conservative Interface Flux
Mass And Momentum Conservative Interface Flux
Turbulence Conservative Interface Flux
Boundary - DeswirlOUTLET
Type OUTLET
Location OUTLET
Settings
Flow Regime Subsonic
Mass And Momentum Average Static Pressure
     Pressure Profile Blend  5.0000e-02
     Relative Pressure  1.2075e+02 [kPa]
Pressure Averaging Average Over Whole Outlet
Boundary - HUB_SHR_DESWIRL
Type WALL
Location "HUB, SHROUD, VANE"
Settings
Heat Transfer Fixed Temperature
     Fixed Temperature WallTemp
Mass And Momentum No Slip Wall
Wall Roughness Smooth Wall
Rotor Boundary - Rotor TMS Side 1
Type INTERFACE
Location "CENTER OUTLET 2, CENTER OUTLET 2 10,
CENTER OUTLET 2 11, CENTER OUTLET 2 12,
CENTER OUTLET 2 13, CENTER OUTLET 2 14, CENTER OUTLET 2 15,
 CENTER OUTLET 2 2, CENTER OUTLET 2 3
, CENTER OUTLET 2 4, CENTER OUTLET 2 5, CENTER OUTLET 2 6,
CENTER OUTLET 2 7, CENTER OUTLET 2 8, CENTER OUTLET 2 9"
Settings
Heat Transfer Conservative Interface Flux
Mass And Momentum Conservative Interface Flux
Turbulence Conservative Interface Flux
Boundary - RotorPERINT Side 1
Type INTERFACE
Location CENTER PER 1 2
Settings
Heat Transfer Conservative Interface Flux
Mass And Momentum Conservative Interface Flux
Turbulence Conservative Interface Flux
Boundary - RotorPERINT Side 2
Type INTERFACE
Location CENTER PER 2 2 15
Settings
Heat Transfer Conservative Interface Flux
Mass And Momentum Conservative Interface Flux
Turbulence Conservative Interface Flux
Boundary - Stator Rotor Side 2
Type INTERFACE
Location "CENTER INLET 2, CENTER INLET 2 10, CENTER
INLET 2 11, CENTER INLET 2 12, CENTER INLET 2 13,
 CENTER INLET 2 14, CENTER INLET 2 15, CENTER INLET 2 2,
  CENTER INLET 2 3, CENTER INLET 2 4,
 CENTER INLET 2 5, CENTER INLET 2 6, CENTER INLET 2 7,
  CENTER INLET 2 8, CENTER INLET 2 9"
Settings
Heat Transfer Conservative Interface Flux
Mass And Momentum Conservative Interface Flux
Turbulence Conservative Interface Flux
Boundary - HUB_Counterrot
Type WALL
Location "HUB COUNTERROT, HUB COUNTERROT 10,
HUB COUNTERROT 11, HUB COUNTERROT 12, HUB COUNTERROT 13,
 HUB COUNTERROT 14, HUB COUNTERROT 15,
 HUB COUNTERROT 2, HUB COUNTERROT 3, HUB COUNTERROT 4,
  HUB COUNTERROT 5, HUB COUNTERROT 6, HUB COUNTERROT 7
, HUB COUNTERROT 8, HUB COUNTERROT 9"
Settings
Heat Transfer Fixed Temperature
     Fixed Temperature WallTemp
Mass And Momentum No Slip Wall
     Wall Velocity Counter Rotating Wall
Wall Roughness Smooth Wall
Boundary - HUB_ROTOR
Type WALL
Location "HUB 3, HUB 3 10, HUB 3 11, HUB 3 13, HUB 3 12,
HUB 3 14, HUB 3 15, HUB 3 2, HUB 3 3, HUB 3 4, HUB 3 5,
HUB 3 6, HUB 3 7, HUB 3 8, HUB 3 9"
Settings
Heat Transfer Fixed Temperature
     Fixed Temperature WallTemp
Mass And Momentum No Slip Wall
Wall Roughness Smooth Wall
Boundary - RotorBlade
Type WALL
Location "FILLET HUB, FILLET HUB 10, FILLET HUB 11,
FILLET HUB 12, FILLET HUB 13, FILLET HUB 14, FILLET HUB 15,
FILLET HUB 2, FILLET HUB 4, FILLET HUB 3, FILLET HUB 5,
FILLET HUB 6, FILLET HUB 7, FILLET HUB 8, FILLET HUB 9"
Settings
Heat Transfer Fixed Temperature
     Fixed Temperature WallTemp
Mass And Momentum No Slip Wall
Wall Roughness Smooth Wall
Boundary - SHROUD
Type WALL
Location "CENTER SHROUD, BLADE TIP SHR, BLADE TIP SHR 10,
BLADE TIP SHR 11, BLADE TIP SHR 12, BLADE TIP SHR 13,
BLADE TIP SHR 15, BLADE TIP SHR 14, BLADE TIP
 SHR 2, BLADE TIP SHR 3, BLADE TIP SHR 4, BLADE TIP SHR 5,
 BLADE TIP SHR 6, BLADE TIP SHR 7, BLADE TIP SHR 8,
  BLADE TIP SHR 9, CENTER SHROUD 10,
 CENTER SHROUD 11, CENTER SHROUD 12, CENTER SHROUD 13,
  CENTER SHROUD 14, CENTER SHROUD 15, CENTER SHROUD 2,
 CENTER SHROUD 3, CENTER SHROUD 4, CENTER SHROUD 5,
 CENTER SHROUD 6, CENTER SHROUD 7, CENTER SHROUD 8,
 CENTER SHROUD 9"
Settings
Heat Transfer Fixed Temperature
     Fixed Temperature WallTemp
Mass And Momentum No Slip Wall
     Wall Velocity Counter Rotating Wall
Wall Roughness Smooth Wall
Stator Boundary - StatorInlet
Type INLET
Location "CENTER INLET, CENTER INLET 3, CENTER INLET 4,
CENTER INLET 5, CENTER INLET 6, CENTER INLET 7,
CENTER INLET 8, CENTER INLET 9"
Settings
Flow Direction Normal to Boundary Condition
Flow Regime Subsonic
Heat Transfer Total Temperature
     Total Temperature  4.4400e+02 [K]
Mass And Momentum Total Pressure
     Relative Pressure  4.6000e+00 [bar]
Turbulence Medium Intensity and Eddy Viscosity Ratio
Boundary - Stator Rotor Side 1
Type INTERFACE
Location "CENTER OUTLET, CENTER OUTLET 3,
CENTER OUTLET 4, CENTER OUTLET 5, CENTER OUTLET 6,
 CENTER OUTLET 7, CENTER OUTLET 8, CENTER OUTLET 9"
Settings
Heat Transfer Conservative Interface Flux
Mass And Momentum Conservative Interface Flux
Turbulence Conservative Interface Flux
Boundary - StatorPERINT Side 1
Type INTERFACE
Location CENTER PER 1 9
```

```
Settings
Heat Transfer Conservative Interface Flux
Mass And Momentum Conservative Interface Flux
Turbulence Conservative Interface Flux
Boundary - StatorPERINT Side 2
Type INTERFACE
Location CENTER PER 2
Settings
Heat Transfer Conservative Interface Flux
Mass And Momentum Conservative Interface Flux
Turbulence Conservative Interface Flux
Boundary - StatorBlade
Type WALL
Location "VANE 2, VANE 2 2, VANE 2 3, VANE 2 4,
 VANE 2 5, VANE 2 6, VANE 2 7, VANE 2 8"
Settings
Heat Transfer Fixed Temperature
     Fixed Temperature WallTemp
Mass And Momentum No Slip Wall
Wall Roughness Smooth Wall
Boundary - StatorHub
Type WALL
Location "HUB 2, HUB 2 2, HUB 2 3, HUB 2 4, HUB 2 5,
HUB 2 6, HUB 2 7, HUB 2 8"
Settings
Heat Transfer Fixed Temperature
     Fixed Temperature WallTemp
Mass And Momentum No Slip Wall
Wall Roughness Smooth Wall
Boundary - StatorShroud
Type WALL
Location "SHROUD 2, SHROUD 2 2, SHROUD 2 3,
 SHROUD 2 4, SHROUD 2 5, SHROUD 2 6, SHROUD 2 7,
  SHROUD 2 8"
Settings
Heat Transfer Fixed Temperature
     Fixed Temperature WallTemp
Mass And Momentum No Slip Wall
Wall Roughness Smooth Wall
TMS Boundary - Rotor TMS Side 2
Type INTERFACE
Location "INLET, INLET 3, INLET 4, INLET 5, INLET 6, INLET 7"
Settings
Heat Transfer Conservative Interface Flux
Mass And Momentum Conservative Interface Flux
Turbulence Conservative Interface Flux
Boundary - TMS Deswirl Side 1
Type INTERFACE
Location "UPSTREAM_OUTLET, UPSTREAM_OUTLET 2,
 UPSTREAM_OUTLET 3, UPSTREAM_OUTLET 4,
 UPSTREAM_OUTLET 5, UPSTREAM_OUTLET 6"
Settings
Heat Transfer Conservative Interface Flux
Mass And Momentum Conservative Interface Flux
Turbulence Conservative Interface Flux
Boundary - TMSPERINT Side 1
Type INTERFACE
Location FAM20
Settings
Heat Transfer Conservative Interface Flux
Mass And Momentum Conservative Interface Flux
Turbulence Conservative Interface Flux
Boundary - TMSPERINT Side 2
Type INTERFACE
Location FAM21 6
Settings
Heat Transfer Conservative Interface Flux
Mass And Momentum Conservative Interface Flux
Turbulence Conservative Interface Flux
Boundary - TMSblade1
Type WALL
Location BLADE_FILLETS
Settings
Heat Transfer Fixed Temperature
     Fixed Temperature WallTemp
Mass And Momentum No Slip Wall
Wall Roughness Smooth Wall
Boundary - TMSblade2
Type WALL
Location BLADE_FILLETS 2
Settings
Heat Transfer Fixed Temperature
     Fixed Temperature WallTemp
Mass And Momentum No Slip Wall
Wall Roughness Smooth Wall
Boundary - TMSblade3
Type WALL
Location BLADE_FILLETS 3
Settings
Heat Transfer Fixed Temperature
     Fixed Temperature WallTemp
Mass And Momentum No Slip Wall
Wall Roughness Smooth Wall
Boundary - TMSblade4
Type WALL
Location BLADE_FILLETS 4
Settings
Heat Transfer Fixed Temperature
     Fixed Temperature WallTemp
Mass And Momentum No Slip Wall
Wall Roughness Smooth Wall
Boundary - TMSblades
Type WALL
Location "BLADE_FILLETS 5, BLADE_FILLETS 6"
Settings
Heat Transfer Fixed Temperature
     Fixed Temperature WallTemp
Mass And Momentum No Slip Wall
Wall Roughness Smooth Wall
Boundary - TMShub
Type WALL
Location "HUBFILLET, HUBFILLET 2, HUBFILLET 3,
 HUBFILLET 4, HUBFILLET 5, HUBFILLET 6"
Settings
Heat Transfer Fixed Temperature
     Fixed Temperature WallTemp
Mass And Momentum No Slip Wall
Wall Roughness Smooth Wall
Boundary - TMSshroud
Type WALL
Location "SHROUDFILLET, SHROUDFILLET 2, SHROUDFILLET 3,
 SHROUDFILLET 4, SHROUDFILLET 6, SHROUDFILLET 5"
Settings
Heat Transfer Fixed Temperature
     Fixed Temperature WallTemp
Mass And Momentum No Slip Wall
Wall Roughness Smooth Wall
```